https://doi.org/10.5194/essd-2023-82
Preprint. Discussion started: 22 March 2023


Open Access Earth System Science Data Discussions

# A Database of Aircraft Measurements of Carbon Monoxide (CO) with High Temporal and Spatial Resolution during 2011 – 2021

Chaoyang Xue[1], Gisèle Krysztofiak[1], Vanessa Brocchi[1], Stéphane Chevrier[1], Michel Chartier[1], Patrick Jacquet[1], Claude Robert[1], Valéry Catoire[1]*

[1]Laboratoire de Physique et Chimie de l'Environnement et de l'Espace (LPC2E), CNRS – Université Orléans – CNES (UMR 7328), 45071 Orléans cedex 2, France

Correspondence: Valéry Catoire (valery.catoire@cnrs-orleans.fr)

**Abstract**

To understand tropospheric air pollution at regional and global scales, the SPIRIT airborne instrument (SPectromètre Infra-Rouge In situ Toute altitude) was developed and used on aircraft to measure volume mixing ratios of carbon monoxide (CO), an important indicator of air pollution, during the last decade. SPIRIT could provide high-quality CO measurements with 1σ precision of 0.3 ppbv at a time resolution of 1.6 s thanks to the coupling of a quantum cascade laser to a Robert multi-pass cell. It can be operated on different aircraft such as Falcon-20 and ATR-42 from DLR (Germany) and SAFIRE (CNRS-CNES-Météo France). With support from various projects, more than 200 flight hours measurements were conducted over three continents (Europe, Asia, and Africa), including two inter-continental measurements (Europe-Asia and Europe-Africa). Levels of CO and its horizontal and vertical distribution are briefly discussed and compared between different regions/continents. CO generally decreases with altitude except for the measurements in high-latitude regions, indicating the important contribution of long-distance transport to CO levels at high-latitude regions. A 3D trajectory mapped by CO level was plotted for each flight and presented in this study. The database is archived on the AERIS database (https://doi.org/10.25326/440), the French national center for atmospheric observations (Catoire et al., 2023). Besides, it could help to validate model performances and satellite measurements. For instance, the database covers measurements at high-latitude regions (i.e., Kiruna, Sweden, 68˚N) where satellite measurements are still challengeable and at low-latitude regions (West Africa and South-East Asia) where in situ data are scarce and satellites need more validation by airborne measurements.

https://doi.org/10.5194/essd-2023-82
Preprint. Discussion started: 22 March 2023


Open Access Earth System Science Data Discussions

## 1 Introduction

The study of atmospheric composition has been widely conducted and understood through comprehensive field campaigns and air quality monitoring networks at the ground level (including mountain summit- and tower- based platforms) in the world (e.g., Acharja et al., 2020; Andreae et al., 2015; Brown et al., 2013; Daellenbach et al., 2020; David et al., 2021; Guo et al., 2014; Hanke et al., 2003; Harrison et al., 2012; Ravi Kant Pathak et al., 2009; Ryerson et al., 2013; Sellers et al., 1995; Shi et al., 2019; Tang et al., 2021). The very recent fifth WHO Air Quality Database (https://www.who.int/data/gho/data/themes/air-pollution/who-air-quality-database, last access: 18 February 2023) compiles ground measurements on air quality for over 6000 cities/human settlements in more than 100 countries. This provides a large body of datasets to understand air quality, its health impacts, and atmospheric chemistry/dynamics in the lower atmosphere as well as its interaction with the biosphere, and to assess model performance in predicting near-ground atmospheric composition. However, those measurements are typically limited to the boundary layer, arising challenges and limitations in understanding regional or global atmospheric processes including chemistry and dynamics since the latter extend well above the surface, indicating the necessity of airborne measurements. Airborne measurements are also necessary for the validation of satellite observations which have undergone fast development and shown important prospects in the past decades. However, measurements at high-latitude regions are still challengeable for satellite, and hence, validation of satellite in those regions are of significant necessity (Hegarty et al., 2022; Wizenberg et al., 2021). Moreover, many important gases are important for atmospheric chemistry, air quality, and global climate but with too low an abundance to be detected by satellite. The vertical profile and regional distribution of those species must be detected by in-situ airborne measurements.

Aircraft serving as a research platform starts in the late 1920s, beginning with meteorological measurements such as temperature and altitude in the UK (Gratton, 2012 and therein). Since the 1940s, scientists have been using aircraft to sample the air to better understand the composition and related processes of the atmosphere far above the surface (https://earthobservatory.nasa.gov/blogs/fromthefield/2016/07/26/long-history-of-using-aircraft-to-understand-the-atmosphere/, last access: 18 February 2023). Owning to the development of rapid-response and high-precision instruments, aircraft measurements become more and more popular, particularly in North America and Europe (Ryerson et al., 2013; Fast et al., 2007; Hamburger et al., 2011; Fehsenfeld et al., 2006; Mallet et al., 2016; Andrés Hernández et al., 2021; Machado et al., 2018; Crawford et al., 2021). In addition to measurements within the boundary layer, the aircraft platform could allow measurements through the troposphere and even reach the lower stratosphere (<20 km above sea level (asl)), through which the atmospheric dynamics and the distribution of pollution at both horizontal and vertical scales could be achieved.

Carbon monoxide (CO) is the second-largest atmospheric carbon compound (after $CO_2$), mainly emitted by incomplete combustion processes, e.g., biomass burning, fossil fuel combustion, etc. Its moderate lifetime of ca. 1-2 months indicates that its abundance is generally impacted by emissions at a regional scale. In a polluted atmosphere such as urban areas, CO is mainly produced from incomplete combustion processes such as coal/gasoline/diesel/biomass combustion and its

https://doi.org/10.5194/essd-2023-82
Preprint. Discussion started: 22 March 2023




concentration could reach levels of several ppmv (Xue et al., 2020; Dekker et al., 2019). In the background atmosphere (e.g., remote areas, marine boundary layer) or the upper troposphere, CO is generally low (<100 ppbv) (Lelieveld et al., 2008) mainly resulting from atmospheric oxidization processes e.g., the oxidation of methane by OH radicals. A high level of CO in a background atmosphere typically indicates impacts of regional transport (or convection/eruption for the upper troposphere) (Krysztofiak et al., 2018). Therefore, aircraft CO measurements can provide an overview of the pollution in the target region and are a good indicator of regional pollution levels and intensive emission events, e.g., wildfires (Jaffe and Wigder, 2012; Jaffe et al., 2022).

Another important utilization of aircraft measurements is the validation of chemical-transport model simulations. Satellite observations are more and more popularly used to study atmospheric composition. Many satellites can detect CO, such as MOPITT (https://terra.nasa.gov/about/terra-instruments/mopitt, last access: 18 February 2023), IASI (https://www.eumetsat.int/iasi, last access: 18 February 2023) and TROPOMI (http://www.tropomi.eu/, last access: 18 February 2023). However, satellite observations of CO need to be validated by measurement at different regions. For instance, recently, Wizenberg et al. (2021) compared CO measurements from TROPOMI, the Atmospheric Chemistry Experiment (ACE) Fourier transform spectrometer (FTS), and a high-Arctic ground-based FTS. They found different biases in different regions, e.g., positive biases (ca. +7%) in northern and southern polar regions and negative biases (ca. -9%) in equatorial regions.

Herein, based on a sensitive airborne instrument (SPIRIT) with high-resolution and high-precision CO detection, seven aircraft campaigns funded by European and French national projects were conducted worldwide between 2011 and 2021, accompanied by two inter-continental measurements. This database summarizes all the data obtained during those aircraft campaigns.

## 2 Method: the SPIRIT Instrument

### 2.1 Set-up

In 2011, an infrared laser absorption spectrometer called SPIRIT (SPectromètre Infra-Rouge In situ Toute altitude) was developed at LPC2E for airborne measurements of trace gases in the troposphere. Details about this instrument can be found in Catoire et al (2017). Briefly, the coupling of a single Robert multi-pass optical cell (with a path length to be adjusted up to 167.78 m) with three interchangeable quantum cascade lasers (QCLs) was designed, which allows selecting trace gases to measure, according to the scientific objectives. Absorptions of the laser radiations by the species in the cell at reduced pressure (<40 h Pa) are quantified using a HgCdTe photodetector cooled by the Stirling cycle, according to the Beer-lambert law. For CO, two absorption rovibrational lines were successively used, namely 2179.772 and 2183.224 $cm^{-1}$, with the functioning conditions for the lasers indicated in Table 1. CO was always measured for all the scientific flights regarding its essential role in atmospheric chemistry, as discussed in Section 1. Hence, in this database, all the airborne CO measurements during the last decade are summarized.

https://doi.org/10.5194/essd-2023-82
Preprint. Discussion started: 22 March 2023




**Table 1: Parameters/performance of the SPIRIT instrument.**

| Years of Meas. | Spectral domain swept ($cm^{-1}$) | Current + ramp (mA) | T_QCL (ºC) | Precision (1σ, ppbv) |
|---|---|---|---|---|
| 2011-2016 | 2179.70-2179.85 | 600 + 13 | -12.5 | 0.3 |
| 2019-2021 | 2183.15-2183.35 | 595 + 15 | -13.2 | 0.3 |

### 2.2 QA/QC (Quality Assurance / Quality Control)

In Catoire et al (2017), laboratory experiments and in-flight intercomparison with other instruments were conducted to assess the performances of SPIRIT and the quality of the data. Besides, for each field campaign, in-flight calibration was also conducted during every flight. It was noted that until 2016 (see Section 3.5), SPIRIT could provide high-quality CO data with a precision of 0.3 ppbv (1σ) and an overall uncertainty of less than 1 ppbv, when we perform regular in-flight calibration vs. WMO standard. This is still the case since 2016. As an example, in Section 3.7, we present data with in-flight calibrations.

## 3 Results and Discussion

During the 2011-2021 period, SPIRIT was used in 7 aircraft campaigns with 74 scientific flights. In total, 208.8 hours of in-flight CO measurements were obtained (Table 2). Except for the SHIVA winter campaign, all campaigns were conducted in late spring or summer. In general, most campaigns were conducted in Europe except for the SHIVA and the DACCIWA campaigns conducted in Southeast Asia and West Africa, respectively. A wide area was covered by the measurements, for example, including tropical regions (SHIVA and DACCIWA) and northern mid-latitude regions (all others). Measurements during the MAGIC 2021 also cover a part of the northern high-latitude region. It is worth noting that two inter-continental flights, one from Europe to South Asia and the other from Europe to West Africa, were conducted during the transition flights for SHIVA and DACCIWA projects (more details in Section 3.9).

https://doi.org/10.5194/essd-2023-82
Preprint. Discussion started: 22 March 2023


Open Access Earth System Science Data Discussions

**Table 2: Information about SPIRIT CO measurements.**

| Projects | Period | Aircraft | Number of Flights | Region | Duration (h) |
|---|---|---|---|---|---|
| SHIVA (2011) | Nov. – Dec. 2011 | A | 16 | 1° – 8° N, 114° – 122° E | 58.5 |
| SHIVA (2011)[a] | Nov. 2011 | A | 5 | 4° – 49° N, 11° – 115° E | 17.0 |
| TC2 (2013) | Mar. – May 2013 | B | 11 | 40° – 48° N, -8° – 9° E | 26.8 |
| ChemCalInt (2014) | May 2014 | C | 4 | 42° – 46° N, 0° – 6° E | 13.9 |
| GLAM (2014) | Aug. 2014 | B | 9 | 33° – 46° N, -1° – 35° E | 24.3 |
| Test sur ATR-42 (2016) | May 2016 | C | 1 | 42° – 44° N, 0° – 2° E | 2.3 |
| DACCIWA (2016) | Jun. – Jul. 2016 | A | 14 | 3° – 11° N, -5° – 3° E | 51.7 |
| DACCIWA (2016)[b] | Jun. 2016 | A | 5 | 5° – 52° N, -18° – 13° E | 13.3 |
| MAGIC (2019) | Jun. 2019 | B | 3 | 43° – 49° N, -2° – 4° E | 9.7 |
| MAGIC (2021) | Aug. 2021 | C | 6 | 64° – 69° N, 6° – 27° E | 21.4 |
| Total | | | **74** | | **208.8** |

[a]: 5 inter-continent flights from Europe to Asia; [b]: 5 inter-continental flights from Europe to Africa.

A: Falcon-20 DLR; B: Falcon-20 SAFIRE; C: ATR-42 SAFIRE

### 3.1 SHIVA – Malaysia (2011)

In the framework of the SHIVA (**S**tratospheric Ozone: **H**alogen **I**mpacts in a **V**arying **A**tmosphere) project of the European Commission FP7-Enviroment Program (https://cordis.europa.eu/project/id/226224, last access: 18 February 2023), 16 research flights were conducted using the German Aerospace Agency (DLR) Falcon-20 aircraft in Malaysia (Borneo island) between 16 November and 11 December 2011. The three-dimensional trajectories with CO volume mixing ratios (vmr) are displayed in the Supplementary Information in Figures S1 to S16. Measurements during the 5 inter-continental flights from Europe to Asia are presented in Section 3.9.

The SPIRIT instrument was on board during all the flights (58.5 hours) for measurements of CO vmr. Figure 1 shows all the trajectories of those flights. Most measurements were conducted along the coastal lines of Malaysia and Brunei, with several flights reaching the hinterland of this island and several flights crossing the South China Sea and reaching the region of Malacca Strait. The measurement domain represents a typical tropical region (latitude scale: 1° -7° N)

https://doi.org/10.5194/essd-2023-82
Preprint. Discussion started: 22 March 2023


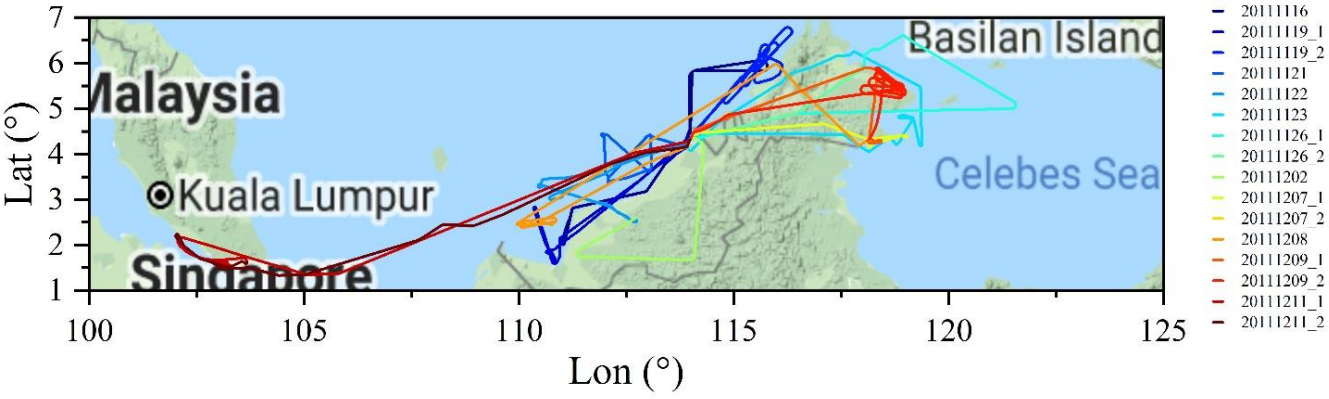


**Figure 1: Flight trajectories during the SHIVA 2011 campaign. Map copyright: © GoogleMap.**

Figure 2 exhibits the trajectory of the first scientific flight on 19 November 2011. The aircraft took off from Miri airport (Malaysia), gradually increasing its altitude to 8400 m asl. It flew along the coastal line of the Sarawak state (Malaysia) and reduced its flying height before reaching the southwest of the Sarawak state. Then, after conducting horizontal measurements over the ocean boundary layer, the aircraft increased its flying height and flew back to Miri airport. After about 2.4 hours of measurements, the aircraft landed at Miri airport. During the flight, the observed CO was within the range of 60-140 ppbv

The polluted air in the boundary layer can also be lifted by convection to affect the upper troposphere. For instance, based on the measurements on flights referenced as 20111119b, 20111209, 20111211_1, and 20111211_2 in the SHIVA project, Krysztofiak et al. (2018) found correlated enhancements of CO, $CH_4$, and short-lived halogen species (i.e., $CH_3I$ and $CHBr_3$) at heights around 11-13 km asl, which is interpreted as the fingerprint of the vertical transport from the boundary layer driven by the convective updraft. The fraction of air mass from the boundary layer can reach 67%, indicating the significant impact of the convective system on the composition of the upper troposphere in the tropical regions (Hamer et al., 2013, 2021).

https://doi.org/10.5194/essd-2023-82
Preprint. Discussion started: 22 March 2023


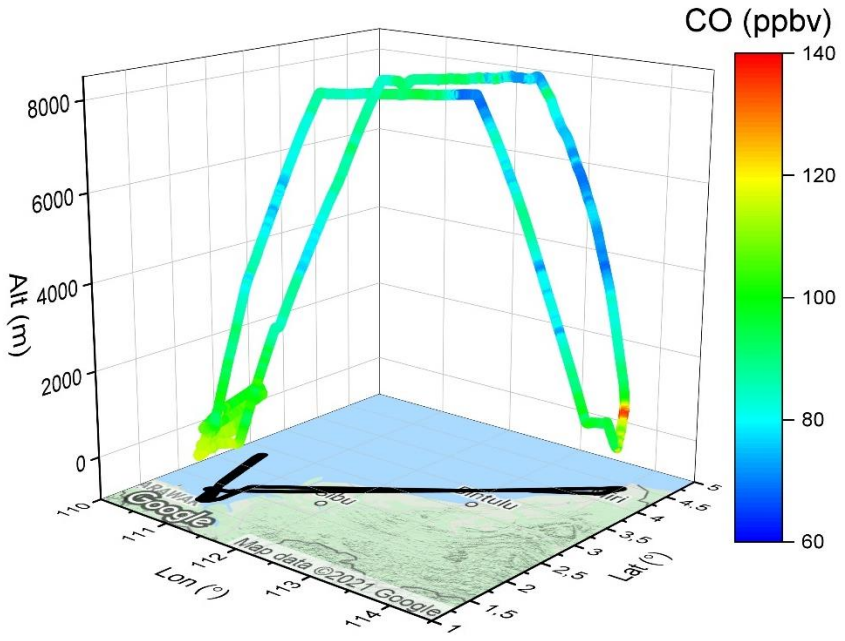


**Figure 2: Flight trajectory colored by CO levels on flight-20111119_1. Map copyright: © GoogleMap.**

### 3.2 Traînées de Condensation et Climat: TC2 - France (2013)

In the framework of the contrails and climate project TC2 (Traînées de Condensation et Climat, http://www.cerfacs.fr/TC2/index.html, last access: 18 February 2023), 11 flight measurements (Figures S17-S27 in the Supplementary Information) were conducted from 12 March to 31 May 2013, with a total measurement duration of around 27 hours. For each flight, the Falcon-20 aircraft with SPIRIT on board flew in the wake of commercial flights, most of which are on the Paris – North Africa route. This allows the detection of aircraft emissions and the study of the air mass aging of contrails. As shown in Figure 3, most measurements were conducted in the region over Toulouse and the South West of France, but several flights reached the Atlantic Ocean and the Mediterranean Sea.

Figure 4 shows the measurements during the 20 March 2013 flight, since they are at the heart of the study, i.e., the emissions of $NO_2$ and CO by aircraft. Sudden increases of $NO_2$ by a few ppb (from a background level of less than 0.5 ppb) were observed when chasing aircraft a few minutes in the wake behind them, but no increase of CO as seen here in the middle of ceiling altitude (10.5 km), suggesting complete combustion in the aircraft engines.

https://doi.org/10.5194/essd-2023-82
Preprint. Discussion started: 22 March 2023


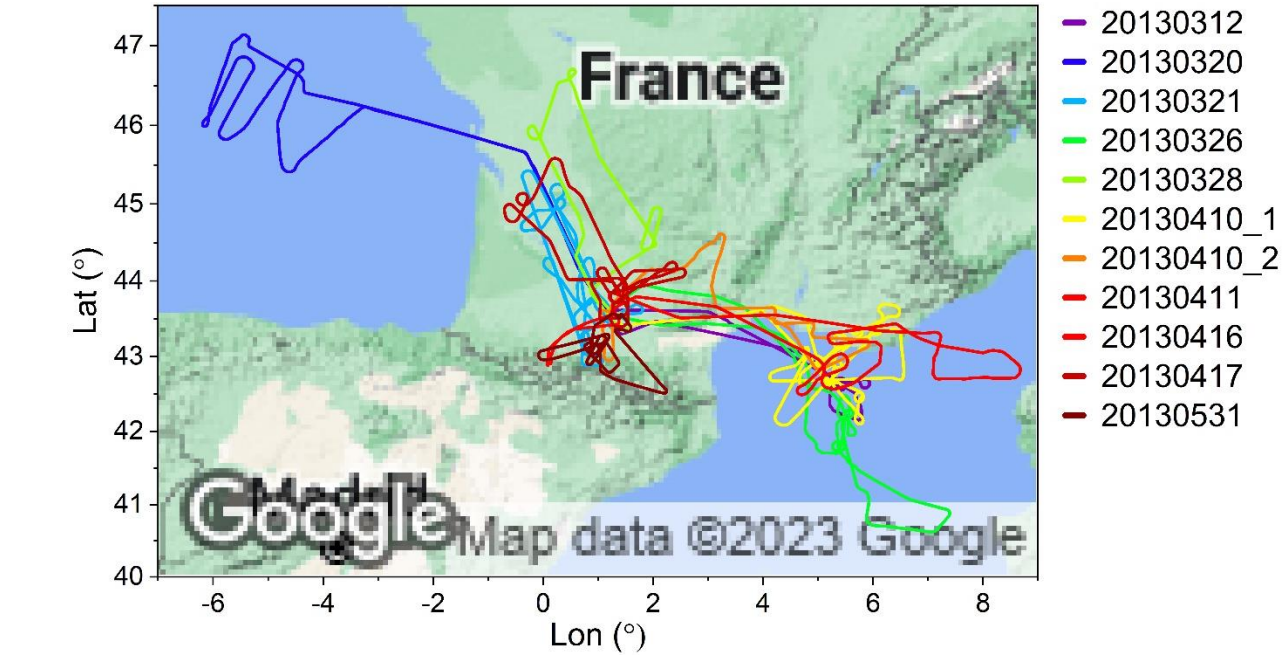


**Figure 3: Flight trajectories during the TC2 2013 campaign. Map copyright: © GoogleMap.**

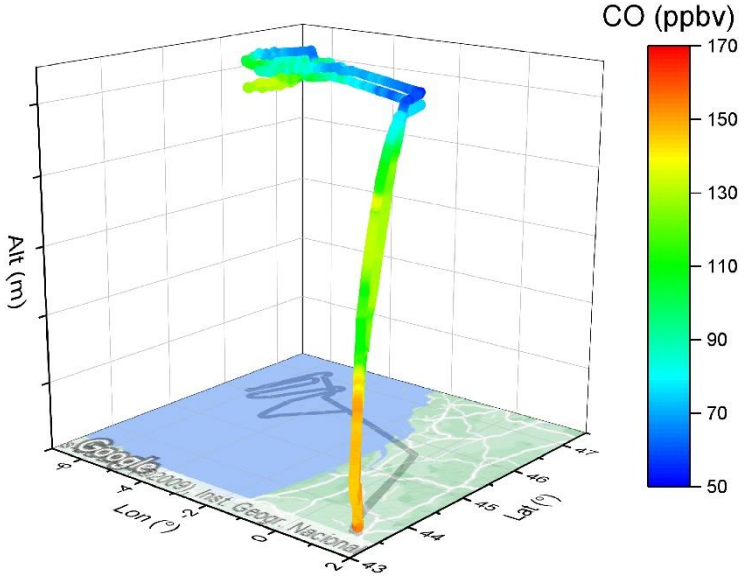


155

**Figure 4: Flight trajectory colored by CO levels on flight-20130320_1. Map copyright: © GoogleMap.**

https://doi.org/10.5194/essd-2023-82
Preprint. Discussion started: 22 March 2023




### 3.3 ChemCalInt - France (2014)

The ChemCalInt project, a French initiative part of the European JRA TGOE in EUFAR for the traceability in gas-phase observations' on-board research aircraft, was designed to intercompare CO and $CH_4$ analyzers for use in French airborne campaigns. Figure 5 shows all the flight trajectories during this project. Four flights were conducted in southern France, generally between/around Toulouse, Clermont-Ferrand, and the Pyrenees Mountains (Figures S28-S31). This project was built to compare the measurements of CO and $CH_4$ by different instruments in order to ensure their consistency and their performance and to implement adapted calibration procedures in future campaigns.

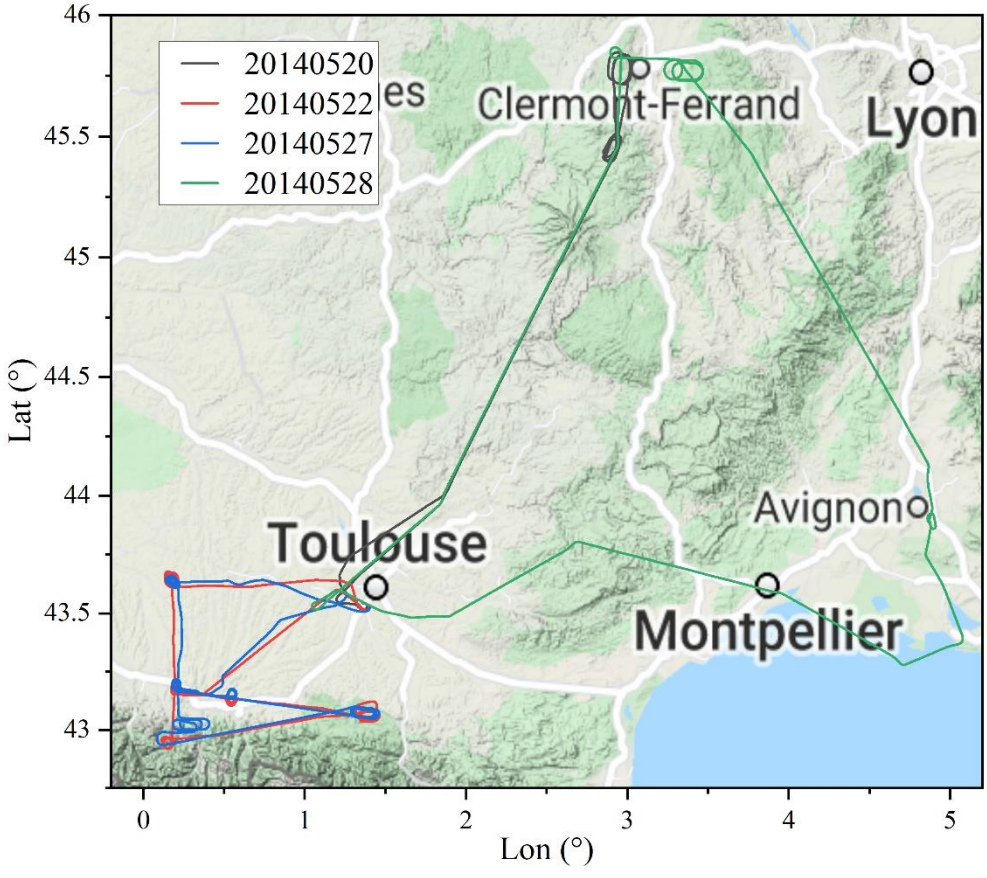


**Figure 5: Flight trajectories during the ChemCallnt 2014 campaign. Map copyright: © GoogleMap.**

In Figure 6, CO measurements along with the flight trajectories are shown. The aircraft flew to the meteorological station of Peyrusse-Vieille, the Centre de Recherches Atmosphériques de Lannemezan (OMP), the Pyrenees National Park, and the Regional Natural Park of the Ariegean Pyrenees. Over this natural park, a background measurement of the vertical profile of CO (i.e. < 115 ppbv) was conducted. In general, the measured CO vmr during this flight was lower than 120 ppbv, with an

https://doi.org/10.5194/essd-2023-82
Preprint. Discussion started: 22 March 2023




exception over Toulouse. This is the typical CO level in Southwest France with no big cities and no significant anthropogenic emissions in this region. The vertical homogeneity of CO over the Regional Park is representative of CO distribution over this region as seen in Section 3.9 and Figure 25.

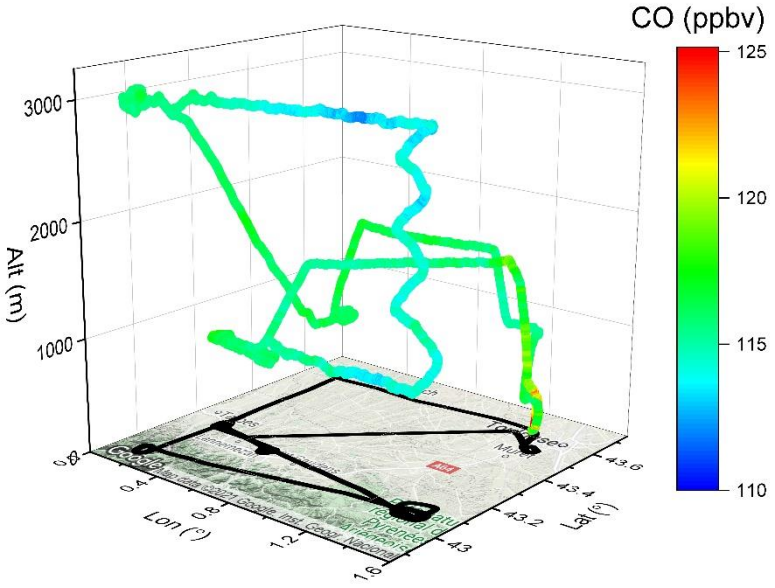


**Figure 6: Flight trajectory colored by CO levels on flight-20140522_1. Map copyright: © GoogleMap.**

### 3.4 ChArMEx – GLAM Mediterranean (2014)

Within the frame of the MISTRALS-ChArMEx program (https://programmes.insu.cnrs.fr/mistrals/programmes/charmex/, last access: 18 February 2023), the GLAM experiment (**G**radient in **L**ongitude of **A**tmospheric constituents above the **M**editerranean basin, https://www.safire.fr/content_page/32-campagnes-passees/106-glam.html?lang=fr, last access: 18 February 2023) aims to describe the high-resolution horizontal and vertical distribution of pollutants over the Mediterranean Basin along an East-West axis (Ricaud et al., 2018; Brocchi et al., 2018). As shown in Figure 7, the measurement domain of the 9 flights covers the target region, west from the France-Spain border and east to Cyprus (Figures S32-S40). Measurements were mostly conducted over the sea, with some exceptions for islands including Balearic Island, Sardinia Island, Crete Island, and Cyprus Island, drawing the whole picture of CO profiles over the Mediterranean Basin. As an example, Figure 8 shows measurements over Cyprus and surrounding regions. High levels of CO up to 130 ppbv were observed in the boundary layer (< 2000 m) over the coastal regions of south-eastern Cyprus and the ocean on the west of Cyprus, indicating impacts of anthropogenic and ship emissions, respectively.

https://doi.org/10.5194/essd-2023-82
Preprint. Discussion started: 22 March 2023


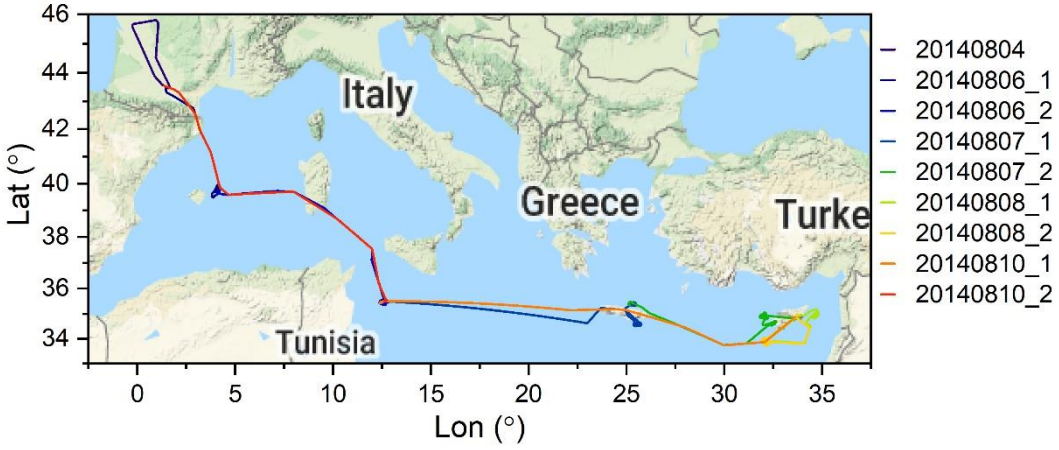


**Figure 7: Flight trajectories during the GLAM-2014 campaign. Map copyright: © GoogleMap.**

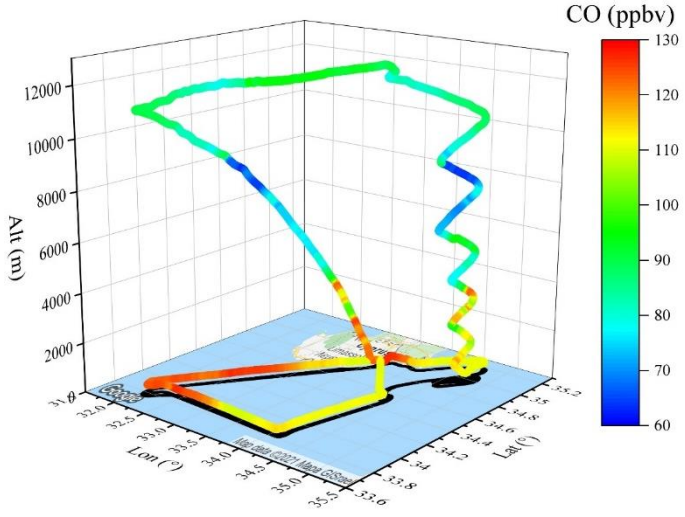


**Figure 8: Flight trajectory colored by CO levels on flight-20140808_1. Map copyright: © GoogleMap.**

### 3.5 Test-ATR-42 (2016)

The Test-ATR-42 project aims to test the performances of SPIRIT, with more intensive calibrations during the flight compared to other field campaigns, as detailed in Catoire et al. (2017). As shown in Figure 9, 17 calibrations with the WMO CO standard of 136.1 ± 0.4 ppbv were made during the flight on 5 February 2016. Those calibrations cover both ascending and descending of the aircraft in the altitude range of 0 – 6 km, showing no dependence of the results on temperature or pressure. Each time the sampling inlet is connected to the standard, measurements rapidly (in 10 s) reach a stable value around 140 ppbv, with a small scattering (< 1 ppbv at 1σ, Figure 10), highlighting the accuracy and reproducibility of SPIRIT in aircraft measurements.

https://doi.org/10.5194/essd-2023-82
Preprint. Discussion started: 22 March 2023




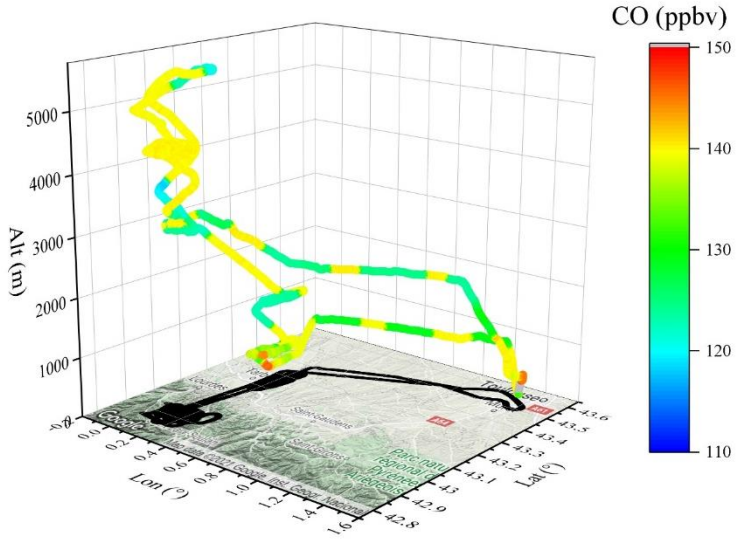


**Figure 9: Flight trajectory colored by CO levels on flight-20160205_1. Map copyright: © GoogleMap.**

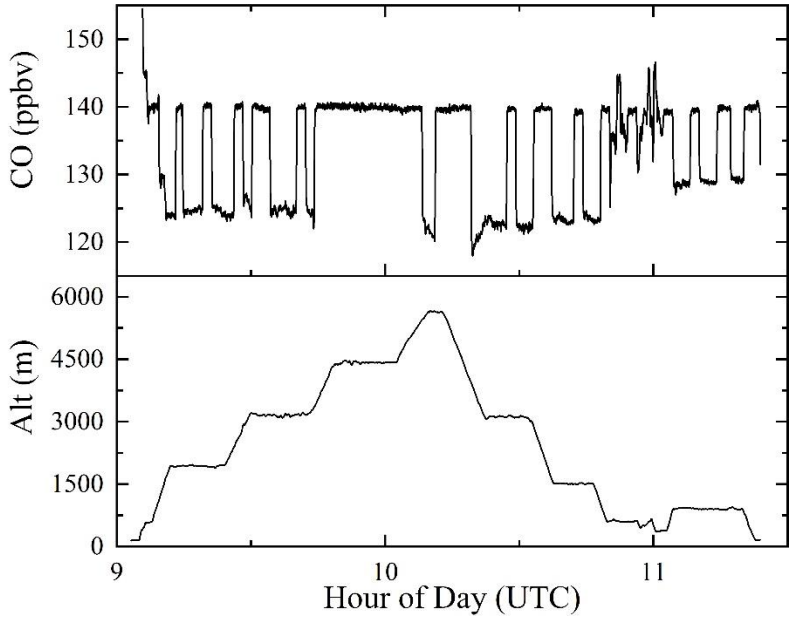


**Figure 10: Time series of CO and altitude on flight-20160502_1.**

### 3.6 DACCIWA – West Africa (2016)

In the summer of 2016, the FP7 EU project DACCIWA (Dynamics-Aerosol-Chemistry-Cloud Interactions in West Africa) was implemented to investigate the atmospheric impacts of anthropogenic and natural emissions in West Africa, where high-

https://doi.org/10.5194/essd-2023-82
Preprint. Discussion started: 22 March 2023




quality airborne measurements are quite scarce (Knippertz et al., 2015; Taylor et al., 2019). 14 flights (> 50 h measurements; Figures S42-S55) were conducted in coastal regions as well as the surrounding Atlantic Ocean and continental regions of West Africa (Figure 11). In general, CO levels in West Africa are higher than those in the Mediterranean Basin (Section 3.4). For example, Figure 12 shows a flight along the coastal lines and over the Gulf of Guinea. High CO values (200 – 300 ppbv) were observed within 2 km above Lomé (capital of Togo), suggesting anthropogenic emissions and/or ship emissions (see ship positions near the Lomé port in Figure S65). Moreover, Brocchi et al. (2019) found that offshore oil rig emissions (e.g., CO, $NO_x$, and aerosol within the boundary layer) also showed an impact on regional air quality. The pollutants emitted above the ocean by ships and oil rigs are thus transported along the West African Monsoon (south-westerly in summer) to the continents (Kniffka et al., 2019; Brocchi et al., 2019), affecting the air quality in those regions. Notably, a pollution plume, with aerosols visible live through the aircraft window and higher CO levels (150 – 200 ppbv) than the background (100 – 150 ppbv, Figure 12), was observed at 2.8 – 4.0 km and was captured again at a similar altitude but further from the coast, which is caused by biomass burning emissions.

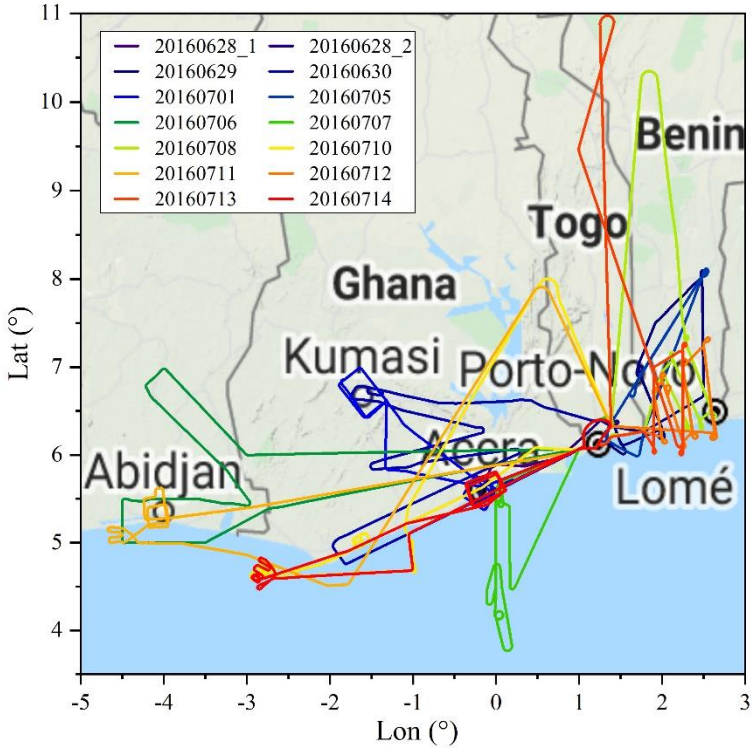


**Figure 11: Flight trajectories during the DACCIWA 2016 campaign. Map copyright: © GoogleMap.**

https://doi.org/10.5194/essd-2023-82
Preprint. Discussion started: 22 March 2023




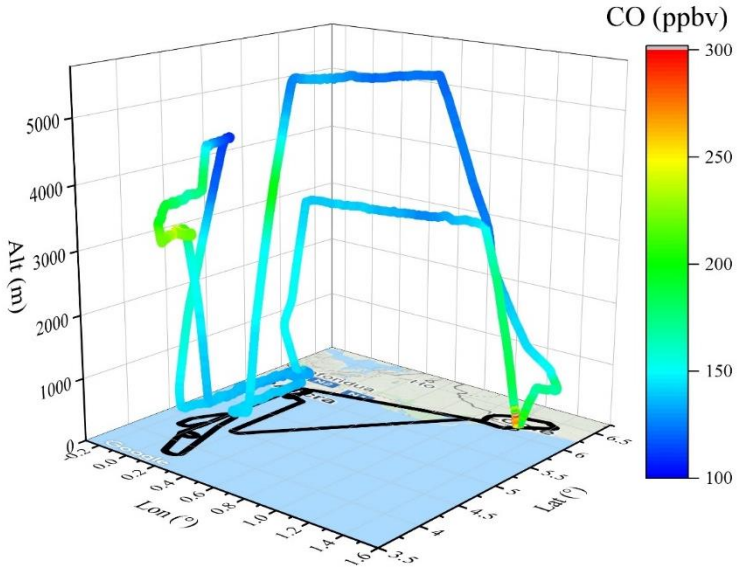


**Figure 12: Flight trajectory colored by CO levels on flight-20160707_1. Map copyright: © GoogleMap.**

Local emissions were frequently observed during this campaign. For instance, as shown in Figure 13, the flight on 12 July 2016 allowed intensive measurements between Lomé (Togo) and Porto-Novo (Benin). Most measurements over the continent showed higher CO levels than those over the ocean, with several CO peaks up to 200 ppbv occasionally accompanied by peaks of $NO_2$ and $SO_2$ (not shown). Those peaks were observed within the boundary layer, indicating the impact of anthropogenic emissions in this region. These measurements are important for documenting and understanding local air pollution, considering that the increasing population and economy lead to more anthropogenic emissions (Knippertz et al., 2015). Also, aerosol pollution traced by CO levels (> 155 ppbv) is shown to slightly enhance atmospheric cooling by low-level clouds in tropical West Africa by increasing the droplet number concentration and reducing the droplet size in the clouds (Hahn et al., 2023; Taylor et al., 2019).

https://doi.org/10.5194/essd-2023-82
Preprint. Discussion started: 22 March 2023




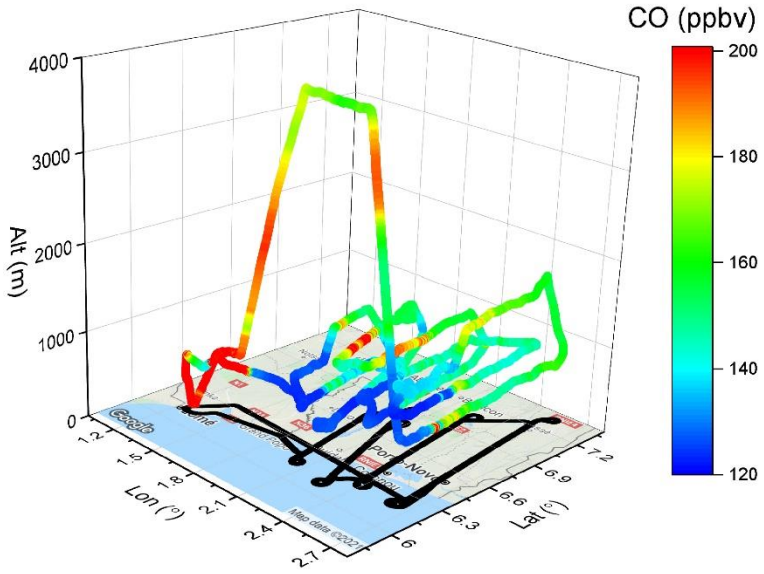


**Figure 13: Flight trajectory colored by CO levels on flight-20160712_1. Map copyright: © GoogleMap.**

### 3.7 MAGIC (2019)

MAGIC (Monitoring Atmospheric composition and Greenhouse gases through multi-Instrument Campaigns, https://magic.aeris-data.fr/, last access: 18 February 2023) is a long-term CNES-CNRS French project, with two main goals: (i) to better understand the vertical exchange of greenhouse gases along the atmospheric column, in connection with atmospheric transport, sources and sinks of the gases at the surface and in the atmosphere; (ii) to contribute to the validation of satellite products of IASI-MetOpC (CNES), Tropomi-Sentinel 5P (ESA), GOSAT 2 (JAXA), and OCO-2 (NASA), and to prepare the validation of space missions MicroCarb, IASI-NG (CNES), and Merlin (CNES-DLR) dedicated to the monitoring of greenhouse gases and other species. In June 2019, the MAGIC campaign was conducted in France, with three flights over the Toulouse-La Rochelle-Orléans-Clermont-Ferrand region (Figure 14 and Figures S56-S58 for 3D trajectories with CO vmr).

Similar to the Test-ATR project (Section 3.5), intensive in-flight calibrations were conducted, which led to the plots of CO versus flight trajectories (Figures S56 – S58). Figure 15 shows the measurements during calibration for the two flights on 18 June 2019. The eight calibration processes cover ascending, descending, and cruise processes in the altitude range of 0 – 12 km. This results in an agreement between the WMO CO_X2014A standard and the SPIRIT instrument within 3.2 ± 0.6 ppbv (1σ) out of 149.0 ppbv, confirming the accuracy and stability of SPIRIT for aircraft measurements.

https://doi.org/10.5194/essd-2023-82
Preprint. Discussion started: 22 March 2023




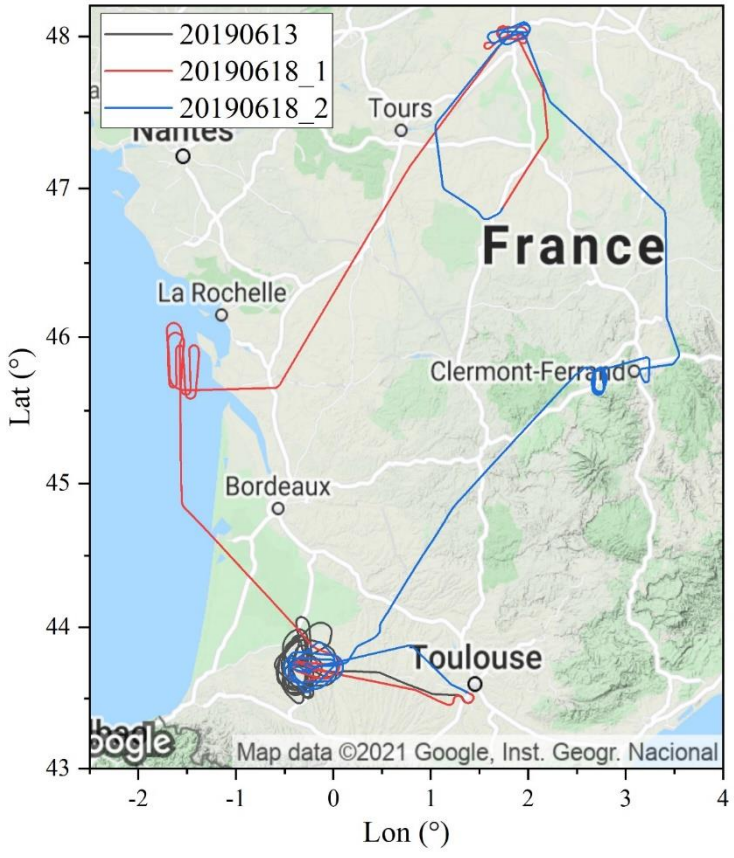


**Figure 14: Flight trajectories during the MAGIC 2019 campaign. Map copyright: © GoogleMap.**

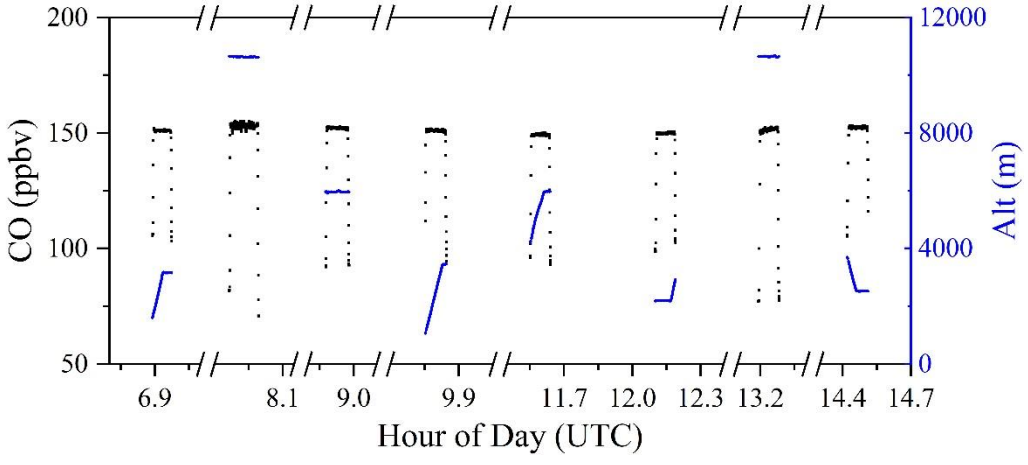


250

**Figure 15: Time series of CO values (black dot) and altitude (blue dot) during calibration on flight- 20190618_1 and 20190618_2.**

https://doi.org/10.5194/essd-2023-82
Preprint. Discussion started: 22 March 2023




### 3.8 MAGIC (2021)

In the continuation of the MAGIC 2019 project above, exploring high latitude regions is of interest since they are warming faster than the global average, as a result of anthropogenic, natural emissions and transport of pollution. However, airborne measurements are scarce in high-latitude regions, which limits the understanding of the horizontal and vertical distribution of pollution and causes problems in validating satellite performance in those regions. In August 2021, the international MAGIC-2021 campaign (https://magic.aeris-data.fr/, last access: 18 January 2023) took place in Kiruna (67.9ºN, 21.1°E), Sweden. As shown in Figure 16, the six flights mainly took measurements over northern Sweden and northern Finland, with one flight reaching the Norwegian Sea (Figures S59-S64).

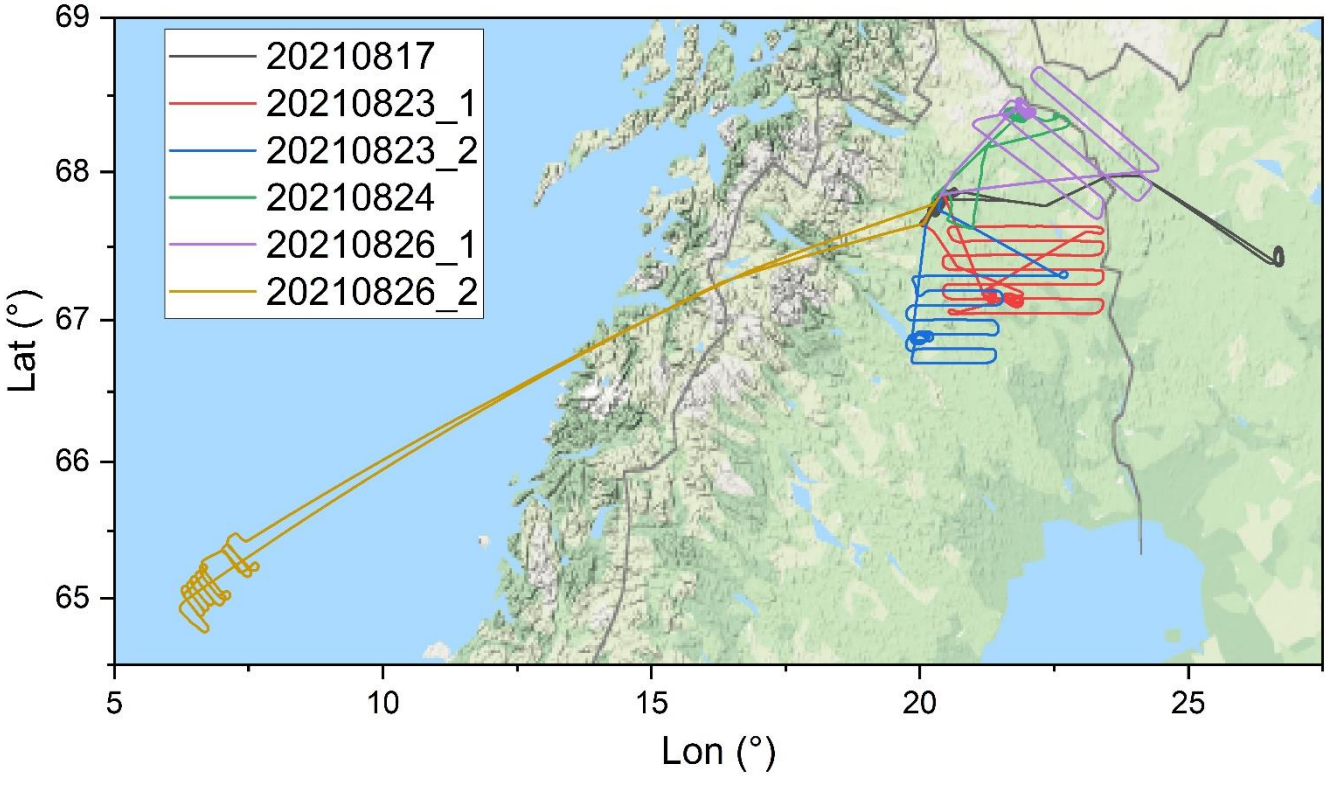


**Figure 16: Flight trajectories during the MAGIC 2021 campaign. Map copyright: © Google Map.**

On the morning of 23 August 2021, an aircraft flight was designed to provide horizontal and vertical measurements that benefit the validation of satellite products aforementioned in Section 3.7. As shown in Figure 17, the aircraft spiraled up, achieving two vertical profiles of measurements within an altitude range of 0 – 7.5 km asl. At the maximum altitude, the aircraft descended to 4.5 km asl and conducted intensive horizontal measurements in the region of 67.0 – 67.6 ºN and 20.0 – 23.5ºE. CO vmr was mostly around 150 – 250 ppbv in this region. After that, it spiraled up again to 7.5 km asl, followed by spiraling down to the ground level before landing back at Kiruna airport. CO was mostly around 150 ppbv within the boundary layer of

https://doi.org/10.5194/essd-2023-82
Preprint. Discussion started: 22 March 2023




~2 km asl. However, it increased with altitude above the boundary layer (peak of 285 ppbv at ~5.5 km asl, Figure 29), likely due to long-range transported fire pollution (study in progress).

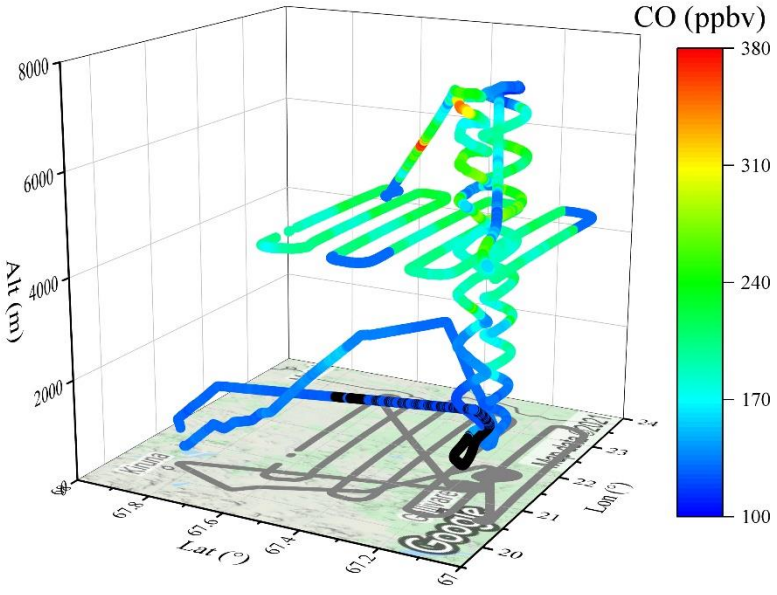


**Figure 17: Flight trajectory colored by CO levels on flight-20210823_1. Map copyright: © Google Map.**

Local emissions from fires were also observed. On 26 August at 9:30 (half an hour after starting the 3.6-hour flight-20210826_1), a fire caused by a rocket engine test occurred at the Swedish Space Corporation Esrange base, which burned parts of the launching facility for sounding rockets and parts of the nearby buildings (red star in Figure 18). The plume of this fire was captured by our measurements. As shown in Figure 18, the aircraft took off at Kiruna airport at around 9:05 a.m. (local time). Around 5 min after the take-off, high CO peaks of more than 200 ppbv were observed at an altitude of 2000 – 2750 m asl, which is nearly above the location of the fire at the Esrange base. The plume was also frequently observed at higher altitudes, i.e., four CO peaks of above 200 ppbv were observed at around 5600 m asl and distributed on a straight line, indicating the widespread of the plume.

https://doi.org/10.5194/essd-2023-82
Preprint. Discussion started: 22 March 2023




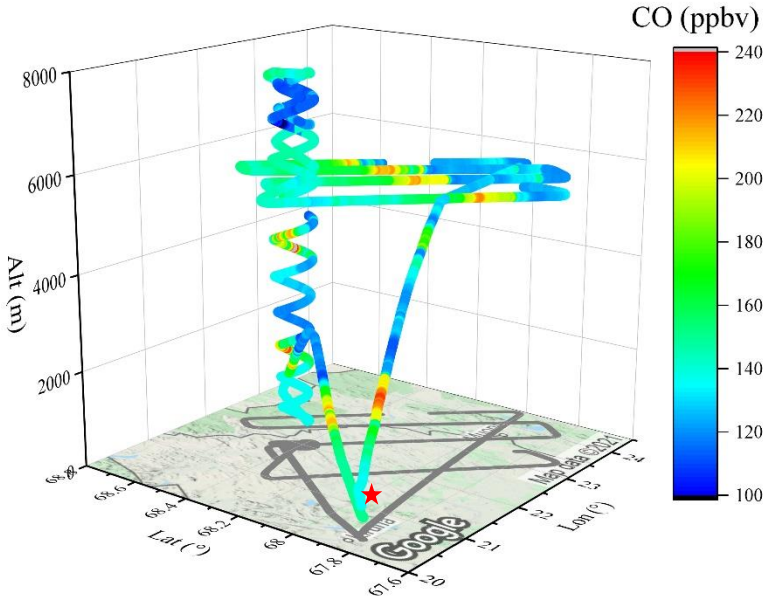


280

**Figure 18: Flight trajectory colored by CO levels on flight-20210826_1. The red star represents the location of the fire at Esrange. Map copyright: © Google Map**

### 3.9 Intercontinental Measurements

Two inter-continental measurements were achieved during SHIVA and DACCIWA projects. Aircraft traveled from Germany to Malaysia in South East Asia in November 2011 and to Ghana in West Africa in June 2016. Except for the landing and take-off, the measurement height was typically constant at a typical cruise altitude of ~10 km asl. This could be used for assessing the performance of chemical transport models and validating satellite observations on a global scale.

285

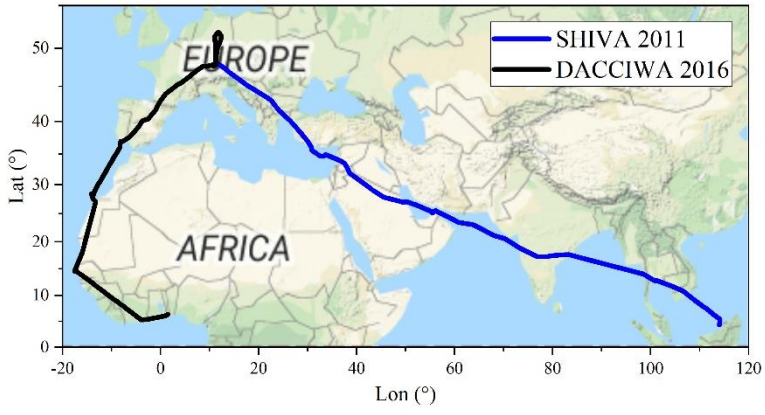


**Figure 19: Trajectories of the two inter-continent flights during the SHIVA 2011 and DACCIWA 2016 campaigns. Map copyright: © Google Map.**

290

https://doi.org/10.5194/essd-2023-82
Preprint. Discussion started: 22 March 2023




### 3.9.1 Europe – Asia

In the framework of SHIVA, an intercontinental measurement was conducted from Munich (Germany) to Miri (Malaysia), with four stops at Larnaca (Cyprus), Dubai, (United Arab Emirates), Hyderabad (India), and Pattaya U-Tapao (Thailand), respectively (Figure 20). Except for CO peaks observed after the take-off, the measured CO was typically lower than 110 ppbv. Higher CO levels (>130 ppbv) were observed in the boundary layer over Hyderabad and U-Tapao, indicating the impacts of local anthropogenic emissions. The pollution of the boundary layer above these last two cities is clearly visible, with CO levels well above 200 ppbv. Also, before landing at Miri, a polluted plume, with significant CO enhancements from around 80 to 200 ppbv, was observed at 10680 m asl. The width of the measured plume was about 630 km, indicating a large emission event and a wide spread. The observed plume may originate from events with intensive emissions, such as wildfires and convective transport (Krysztofiak et al., 2018; Hamer et al., 2021).

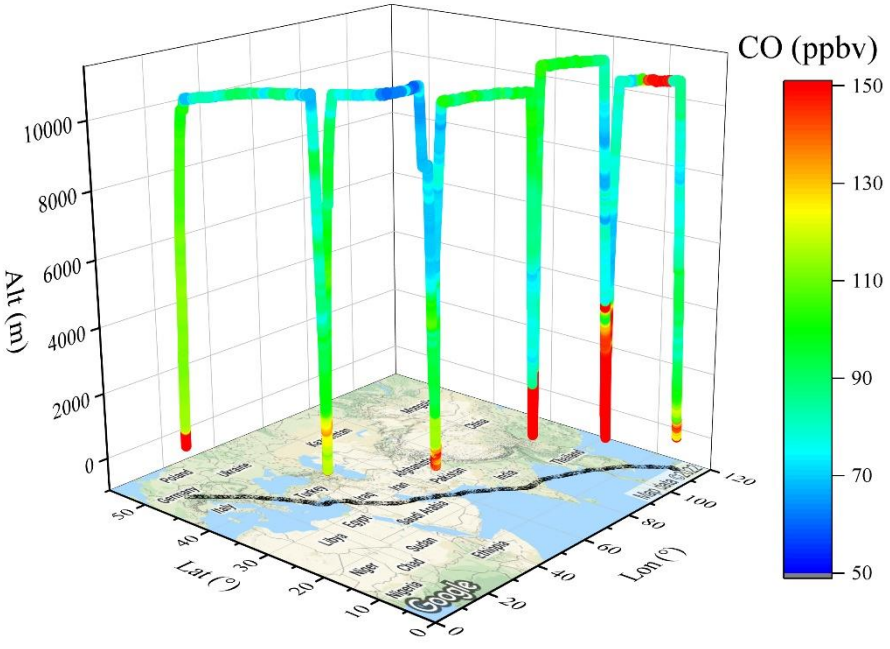


**Figure 20: Flight trajectory colored by CO levels during the inter-continent flight during the SHIVA 2011 campaign. Map copyright: © Google Map.**

### 3.9.2 Europe – Africa

During the DACCIWA project, the SPIRIT instrument was on board the DLR Falcon-20 for measurements during the transit flights from Germany to Togo. There were three stops: Faro (Portugal), Fuerteventura (Canary Island, Spain), and Dakar (Senegal), which allows measurements across West Europe and along the coastal lines of North and West Africa. CO measured over West Europe and North Africa is typically lower than 100 ppbv. However, higher CO levels were observed over West

https://doi.org/10.5194/essd-2023-82
Preprint. Discussion started: 22 March 2023




Africa in the boundary layer and the upper troposphere. For example, before landing at Lomé (Togo), polluted plumes with CO up to 150 ppbv were observed in the altitude range of 20 – 4700 m asl, suggesting strong impacts of regional anthropogenic emissions.

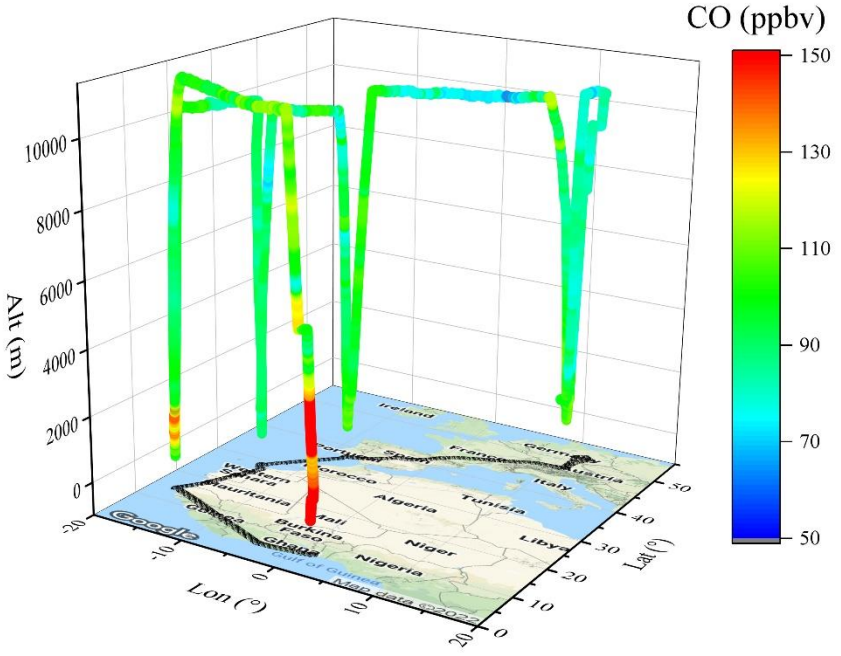


**Figure 21: Flight trajectory colored by CO levels during the intercontinental flight during the DACCIWA 2016 campaign. Map copyright: © Google Map.**

### 3.10 Vertical Profiles of CO in the Different Regions

Figure 22 summarizes the locations of all the measurements presented in this paper, i.e. over three continents (Europe, Asia, and Africa), with two inter-continental measurements (Europe-Asia and Europe-Africa).

https://doi.org/10.5194/essd-2023-82
Preprint. Discussion started: 22 March 2023


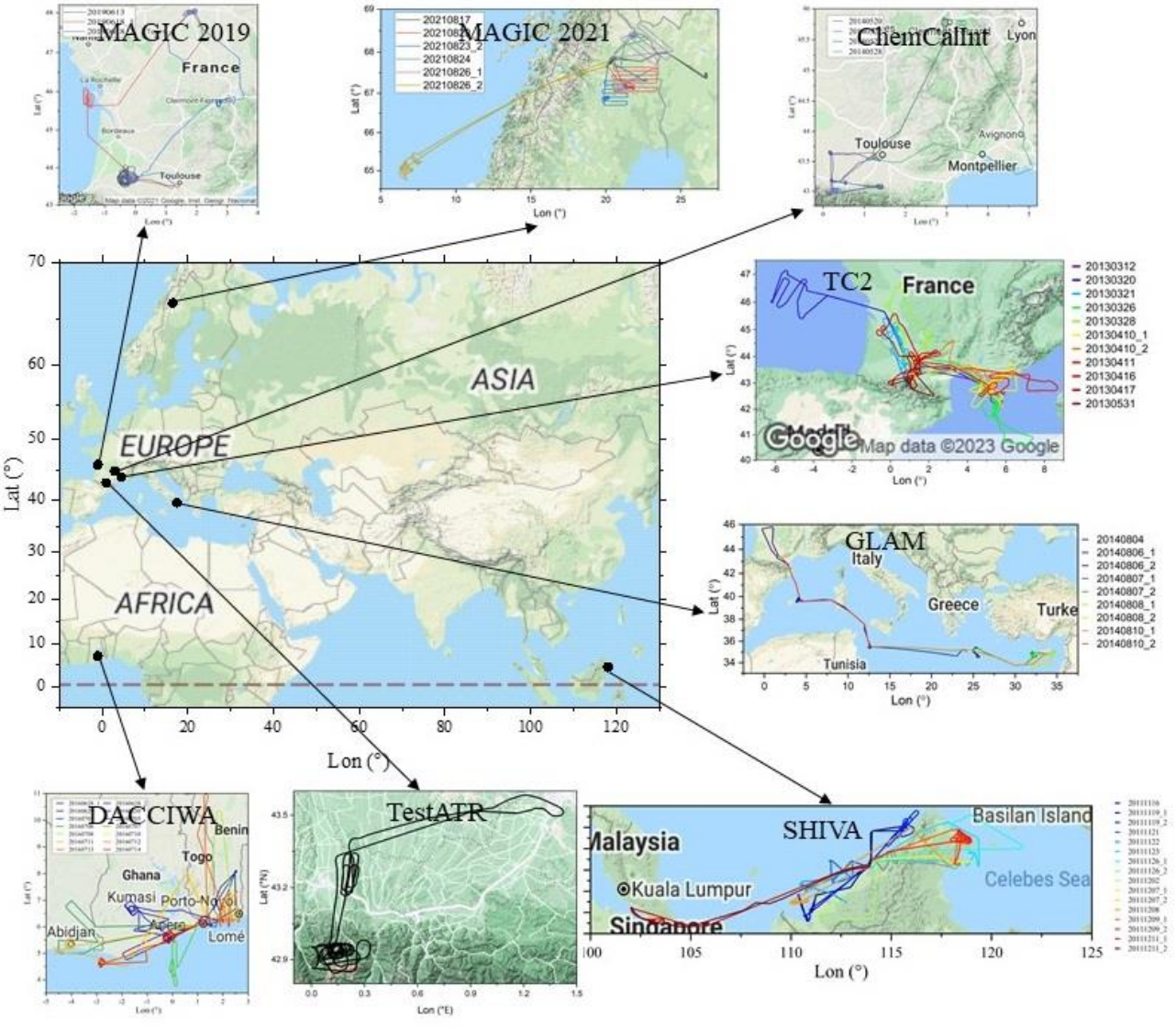


**Figure 22. Locations of all the measurements presented in this paper. Map copyright: © GoogleMap.**

Figure 23 - Figure 29 show the vertical profiles of CO observed during the campaigns. In most cases, CO levels decrease with altitude within the boundary layer (~1-2 km asl) from 100 – 200 ppbv (depending on the region) to lower values in the free troposphere, characterized as such, indicating a strong impact of anthropogenic emissions. Similar observations are made in Alaska where a nearly constant CO value was observed in an altitude range of 0 – 2 km asl (Spackman et al., 2010). However, surface CO vmr in West Africa (Figure 27) is generally in the range of 200 – 300 ppbv. They are higher than in other regions. Indeed, in Europe and the whole Mediterranean region (including TC2-2013, ChemCallnt-2014, and GLAM-2014), most

https://doi.org/10.5194/essd-2023-82
Preprint. Discussion started: 22 March 2023




surface CO levels are lower than 150 ppbv. In southern Asia, surface CO is typically at a similar level to Europe, with exceptions reaching more than 200 ppbv.

Unlike other regions, CO vertical profile measured in high-latitude regions (Kiruna, Sweden) during the MAGIC-2021 campaign increases with altitude, with CO levels of up to 300 ppbv in the altitude range of 5000 – 7000 m asl (Figure 28). CO levels during summer seem similar or higher than inland Europe although a lower anthropogenic emission is expected, suggesting a large contribution from the transport of plumes from wildfires at high latitude regions. Indeed, assimilated TROPOMI satellite observations and CAMS model simulations and reported large CO emissions from wildfires over North America and Russia in July and August 2021, which led to high CO column concentrations in the Arctic region.

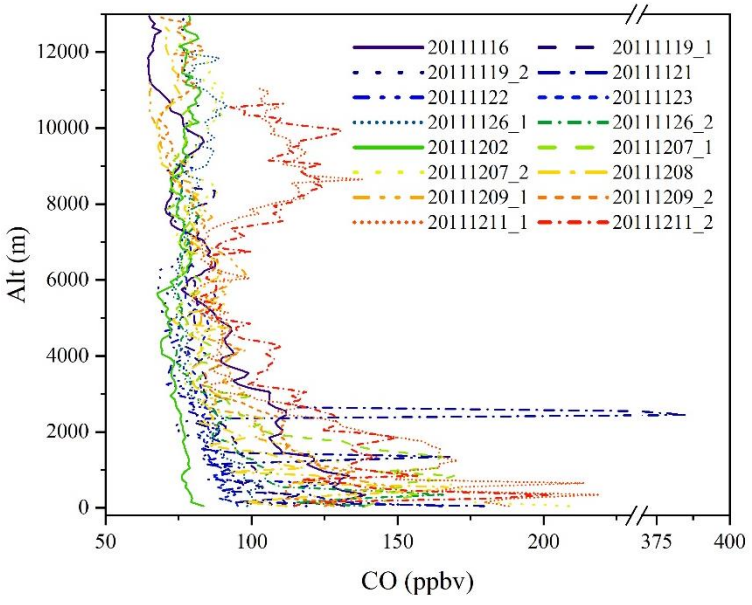


**Figure 23: Vertical profiles of CO of all flights during the SHIVA (2011) campaign. Vertical average bin: 100 m.**

https://doi.org/10.5194/essd-2023-82
Preprint. Discussion started: 22 March 2023




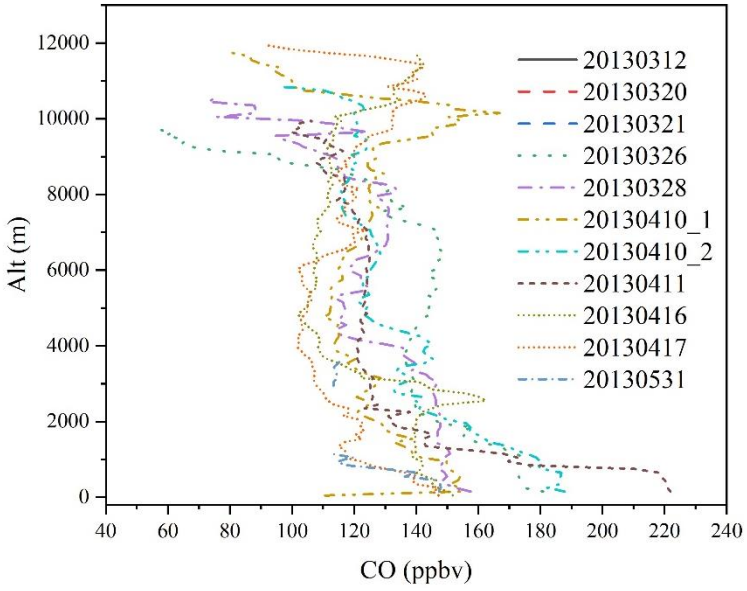


**Figure 24: Vertical profiles of CO of all flights during the TC2 (2013) campaign. Vertical average bin: 100 m.**

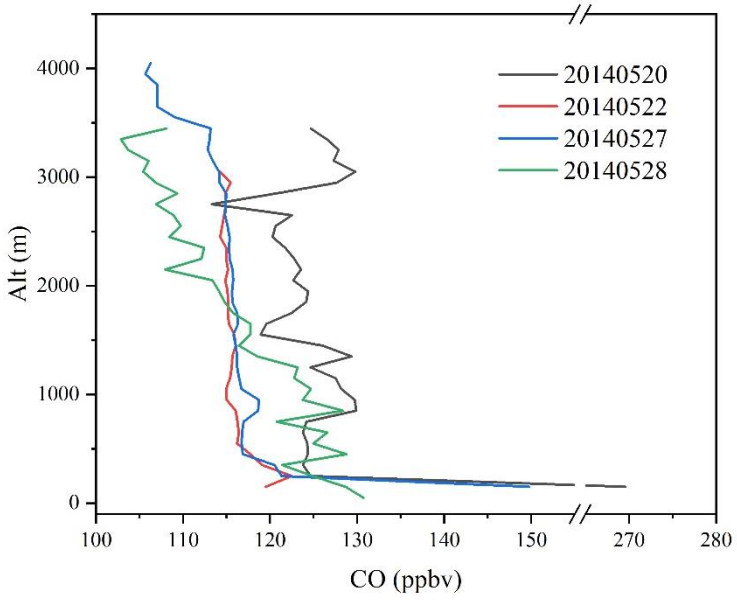


**Figure 25: Vertical profiles of CO of all flights during the ChemCallnt (2014) campaign. Vertical average bin: 100 m.**

340

https://doi.org/10.5194/essd-2023-82
Preprint. Discussion started: 22 March 2023




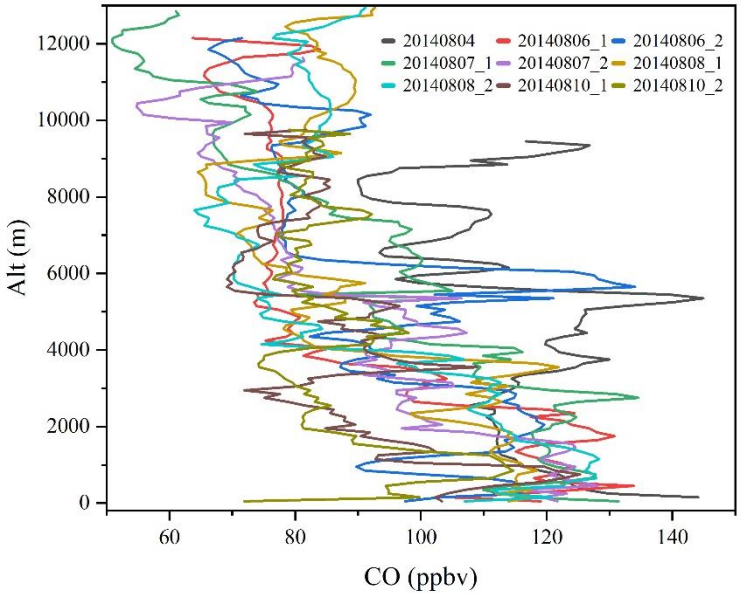


**Figure 26: Vertical profiles of CO of all flights during the GLAM (2014) campaign. Vertical average bin: 100 m.**

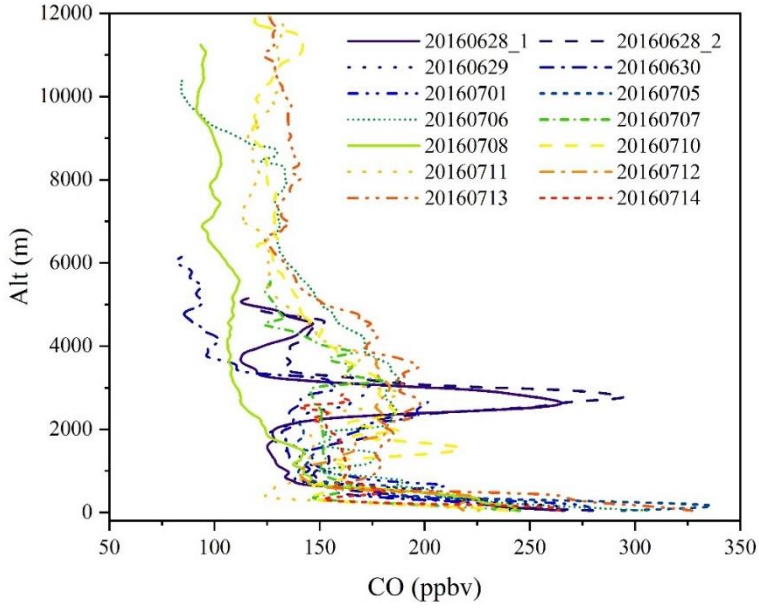


**Figure 27: Vertical profiles of CO of all flights during the DACCIWA (2016) campaign. Vertical average bin: 100 m.**

https://doi.org/10.5194/essd-2023-82
Preprint. Discussion started: 22 March 2023


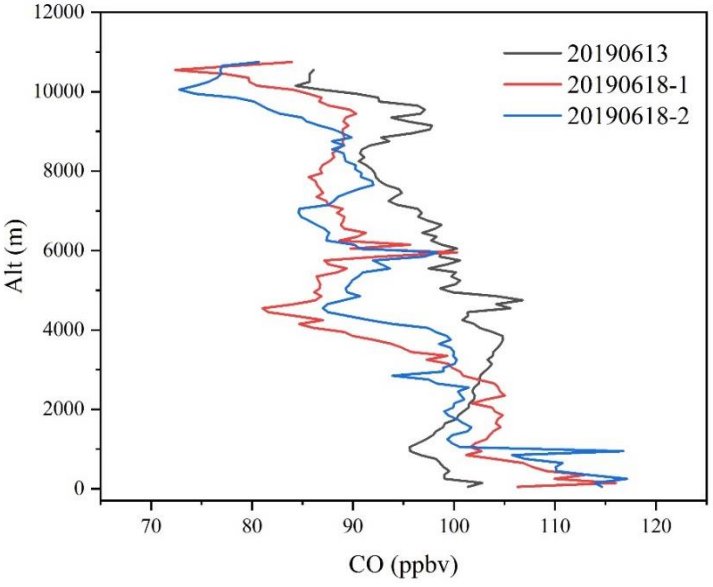


**Figure 28: Vertical profiles of CO of all flights during the MAGIC (2019) campaign. Vertical average bin: 100 m.**

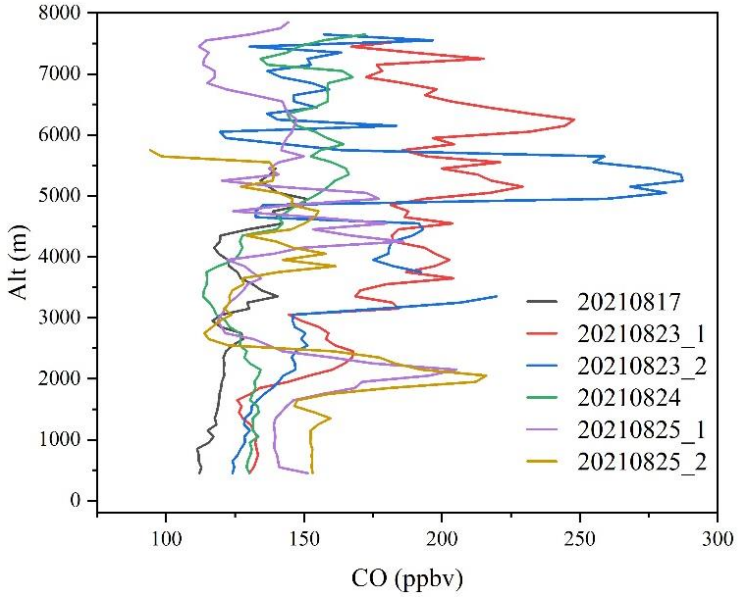


**Figure 29: Vertical profiles of CO of all flights during the MAGIC (2021) campaign. Vertical average bin: 100 m.**

https://doi.org/10.5194/essd-2023-82
Preprint. Discussion started: 22 March 2023



## 4 Data Availability

All the data used in this study are publicly available on the AERIS database (Catoire et al., 2023: https://doi.org/10.25326/440). Any questions concerning this current database or the scheduled SPIRIT aircraft measurements in the future are welcomed by contacting the corresponding author.

## 5 Code Availability

The 3D aircraft trajectories were plotted by OriginPro 2021 (https://www.originlab.com/, last access: 18 February 2023, license needed) and the background maps were inputted by a build-in application (Google Map Import, created by the OriginLab Technical Support, available at https://www.originlab.com/fileExchange/details.aspx?fid=344, last access: 18 February 2023).

## 6 Conclusions

Thanks to the development of the airborne SPIRIT instrument, accurate CO measurements (0.3 ppbv precision at 1σ and overall uncertainty < 4 ppbv) were achieved during the past decade (2011 – 2021). This database describes all aircraft CO measurements by SPIRIT during this period. More than 200 h of airborne measurements were conducted in Europe, South Asia, and West Africa. The measurement domain covers a wide area, including tropical, northern mid-latitude, and northern high-latitude regions. This database also includes two unique intercontinental measurements, one from Germany to Ghana via the West African coast, and the other one from Germany to Malaysia. Many polluted plumes are observed, including anthropogenic emissions, wildfire emissions, convective plumes, and long-distance transport. This database helps to understand such events and to constrain and improve relevant model approaches. Moreover, with the emerging utilization of satellite images, the importance of calibration of those measurements at a regional and/or a global scale becomes more and more significant, revealing the importance of the SPIRIT database.

## 7 Author Contribution

C.X., G.K., and V.C. lead this study. All authors participated in the development, data acquisition, and/or maintenance of SPIRIT during at least one field campaign. All authors commented on and approved this manuscript.

## 8 Competing Interests

The authors declare that they have no competing financial interests.

https://doi.org/10.5194/essd-2023-82
Preprint. Discussion started: 22 March 2023




## 9 Acknowledgments

We are grateful to the LPC2E colleagues Gilles Chalumeau, Thierry Vincent, Kevin Le Letty, Olivier Chevillon, and Anne-Laure Pelé for the mechanical, electronic, and optical development and aircraft campaign support of the SPIRIT instrument, and the Master students Guillaume Robelet and Abdelmalek Bakha (University of Orléans) for their help with the data retrieval and visualization. We thank Hans Schlager (DLR) for facilitating access to SHIVA and DACCIWA projects and the associated Falcon-20 aircraft.

**Funding**: Besides the projects listed in the main text, this work was supported by the PIVOTS project provided by the Region Centre − Val de Loire (ARD 2020 program and CPER 2015 − 2020) and the Labex VOLTAIRE project (ANR-10-LABX-100-01, managed by the University of Orléans). Figure 7

## 10 References

Acharja, P., Ali, K., Trivedi, D. K., Safai, P. D., Ghude, S., Prabhakaran, T., and Rajeevan, M.: Characterization of atmospheric trace gases and water soluble inorganic chemical ions of $PM_1$ and $PM_{2.5}$ at Indira Gandhi International Airport, New Delhi during 2017–18 winter, Sci. Total Environ., 729, 138800, https://doi.org/10.1016/j.scitotenv.2020.138800, 2020.

Andreae, M. O., Acevedo, O. C., Araùjo, A., Artaxo, P., Barbosa, C. G. G., Barbosa, H. M. J., Brito, J., Carbone, S., Chi, X., Cintra, B. B. L., Da Silva, N. F., Dias, N. L., Dias-Júnior, C. Q., Ditas, F., Ditz, R., Godoi, A. F. L., Godoi, R. H. M., Heimann, M., Hoffmann, T., Kesselmeier, J., Könemann, T., Krüger, M. L., Lavric, J. V., Manzi, A. O., Lopes, A. P., Martins, D. L., Mikhailov, E. F., Moran-Zuloaga, D., Nelson, B. W., Nölscher, A. C., Santos Nogueira, D., Piedade, M. T. F., Pöhlker, C., Pöschl, U., Quesada, C. A., Rizzo, L. V., Ro, C. U., Ruckteschler, N., Sá, L. D. A., De Oliveira Sá, M., Sales, C. B., Dos Santos, R. M. N., Saturno, J., Schöngart, J., Sörgel, M., De Souza, C. M., De Souza, R. A. F., Su, H., Targhetta, N., Tóta, J., Trebs, I., Trumbore, S., Van Eijck, A., Walter, D., Wang, Z., Weber, B., Williams, J., Winderlich, J., Wittmann, F., Wolff, S., and Yáñez-Serrano, A. M.: The Amazon Tall Tower Observatory (ATTO): Overview of pilot measurements on ecosystem ecology, meteorology, trace gases, and aerosols, Atmos. Chem. Phys., 15, 10723–10776, https://doi.org/10.5194/acp-15-10723-2015, 2015.

Andrés Hernández, M. D., Hilboll, A., Ziereis, H., Förster, E., Krüger, O., Kaiser, K., Schneider, J., Barnaba, F., Vrekoussis, M., Schmidt, J., Huntrieser, H., Blechschmidt, A.-M., George, M., Nenakhov, V., Klausner, T., Holanda, B., Wolf, J., Eirenschmalz, L., Krebsbach, M., Pöhlker, M., Hedegaard, A., Mei, L., Pfeilsticker, K., Liu, Y., Koppmann, R., Schlager, H., Bohn, B., Schumann, U., Richter, A., Schreiner, B., Sauer, D., Baumann, R., Mertens, M., Jöckel, P., Kilian, M., Stratmann, G., Pöhlker, C., Campanelli, M., Pandolfi, M., Sicard, M., Gomez-Amo, J., Pujadas, M., Bigge, K., Kluge, F., Schwarz, A., Daskalakis, N., Walter, D., Zahn, A., Pöschl, U., Bönisch, H., Borrmann, S., Platt, U., and Burrows, J. P.: Overview: On the transport and transformation of pollutants in the outflow of major population centres – observational data from the EMeRGe European intensive operational period in summer 2017, Atmos. Chem. Phys. Discuss., 1–81, 2021.

Brocchi, V., Krysztofiak, G., Catoire, V., Guth, J., Marécal, V., Zbinden, R., El Amraoui, L., Dulac, F., and Ricaud, P.: Intercontinental transport of biomass burning pollutants over the Mediterranean Basin during the summer 2014 ChArMEx-GLAM airborne campaign, Atmos. Chem. Phys., 18, 6887–6906, https://doi.org/10.5194/acp-18-6887-2018, 2018.

Brocchi, V., Krysztofiak, G., Deroubaix, A., Stratmann, G., Sauer, D., Schlager, H., Deetz, K., Dayma, G., Robert, C., Chevrier, S., and Catoire, V.: Local air pollution from oil rig emissions observed during the airborne DACCIWA campaign, Atmos. Chem. Phys., 19, 11401–11411, https://doi.org/10.5194/acp-19-11401-2019, 2019.

Brown, S. S., Thornton, J. A., Keene, W. C., Pszenny, A. A. P., Sive, B. C., Dubé, W. P., Wagner, N. L., Young, C. J., Riedel, T. P., Roberts, J. M., Vandenboer, T. C., Bahreini, R., Öztürk, F., Middlebrook, A. M., Kim, S., Hübler, G., and Wolfe, D. E.: Nitrogen, Aerosol Composition, and Halogens on a Tall Tower (NACHTT): Overview of a wintertime air chemistry field study in the front range urban corridor of Colorado, J. Geophys. Res. Atmos., 118, 8067–8085, https://doi.org/10.1002/jgrd.50537, 2013.

https://doi.org/10.5194/essd-2023-82
Preprint. Discussion started: 22 March 2023


Catoire, V., Robert, C., Chartier, M., Jacquet, P., Guimbaud, C., and Krysztofiak, G.: The SPIRIT airborne instrument: a three-channel infrared absorption spectrometer with quantum cascade lasers for in situ atmospheric trace-gas measurements, Appl. Phys. B, 123, 244, https://doi.org/10.1007/s00340-017-6820-x, 2017.

Catoire, V., Krysztofiak, G., and Xue, C.: CO measured by SPIRIT during airborne campaigns, [Dataset]. Aeris, https://doi.org/10.25326/440, 2023.

Crawford, J. H., Ahn, J. Y., Al-Saadi, J., Chang, L., Emmons, L. K., Kim, J., Lee, G., Park, J. H., Park, R. J., Woo, J. H., Song, C. K., Hong, J. H., Hong, Y. D., Lefer, B. L., Lee, M., Lee, T., Kim, S., Min, K. E., Yum, S. S., Shin, H. J., Kim, Y. W., Choi, J. S., Park, J. S., Szykman, J. J., Long, R. W., Jordan, C. E., Simpson, I. J., Fried, A., Dibb, J. E., Cho, S. Y., and Kim, Y. P.: The Korea-United States air quality (KORUS-AQ) field study, Elementa, 9, 1–27, https://doi.org/10.1525/elementa.2020.00163, 2021.

Daellenbach, K. R., Uzu, G., Jiang, J., Cassagnes, L., Leni, Z., Vlachou, A., Stefenelli, G., Canonaco, F., Weber, S., Segers, A., Kuenen, J. J. P., Schaap, M., Favez, O., Albinet, A., Aksoyoglu, S., Dommen, J., Baltensperger, U., Geiser, M., El Haddad, I., Jaffrezo, J., and Prévôt, A. S. H.: Sources of particulate-matter air pollution and its oxidative potential in Europe, Nature, 587, 414–419, https://doi.org/10.1038/s41586-020-2902-8, 2020.

David, L. M., Ravishankara, A. R., Brey, S. J., Fischer, E. V, Volckens, J., and Kreidenweis, S.: Could the exception become the rule? "Uncontrollable" air pollution events in the U.S. due to wildland fires, Environ. Res. Lett., 16, 034029, https://doi.org/10.1088/1748-9326/abe1f3, 2021.

Dekker, I. N., Houweling, S., Pandey, S., Krol, M., Röckmann, T., Borsdorff, T., Landgraf, J., and Aben, I.: What caused the extreme CO concentrations during the 2017 high-pollution episode in India?, Atmos. Chem. Phys., 19, 3433–3445, https://doi.org/10.5194/acp-19-3433-2019, 2019.

Fast, J. D., De Foy, B., Rosas, F. A., Caetano, E., Carmichael, G., Emmons, L., McKenna, D., Mena, M., Skamarock, W., Tie, X., Coulter, R. L., Barnard, J. C., Wiedinmyer, C., and Madronich, S.: A meteorological overview of the MILAGRO field campaigns, Atmos. Chem. Phys., 7, 2233–2257, https://doi.org/10.5194/acp-7-2233-2007, 2007.

Fehsenfeld, F. C., Ancellet, G., Bates, T. S., Goldstein, A. H., Hardesty, R. M., Honrath, R., Law, K. S., Lewis, A. C., Leaitch, R., McKeen, S., Meagher, J., Parrish, D. D., Pszenny, A. A. P., Russell, P. B., Schlager, H., Seinfeld, J., Talbot, R., and Zbinden, R.: International Consortium for Atmospheric Research on Transport and Transformation (ICARTT): North America to Europe - Overview of the 2004 summer field study, J. Geophys. Res. Atmos., 111, https://doi.org/10.1029/2006JD007829, 2006.

Gratton, G. B.: The Meteorological Research Flight and its predecessors and successors, J. Aeronaut. Hist., 6, 2012.

Guo, S., Hu, M., Zamora, M. L., Peng, J., Shang, D., Zheng, J., Du, Z., Wu, Z., Shao, M., Zeng, L., Molina, M. J., and Zhang, R.: Elucidating severe urban haze formation in China, Proc. Natl. Acad. Sci., 111, 17373–17378, https://doi.org/10.1073/pnas.1419604111, 2014.

Hahn, V., Meerkötter, R., Voigt, C., Gisinger, S., Sauer, D., Catoire, V., Dreiling, V., Coe, H., Flamant, C., Kaufmann, S., Kleine, J., Knippertz, P., Moser, M., Rosenberg, P., Schlager, H., Schwarzenboeck, A., and Taylor, J.: Pollution slightly enhances atmospheric cooling by low-level clouds in tropical West Africa, Atmos. Chem. Phys. Discuss., 2022, 1–21, https://doi.org/10.5194/acp-2022-795, 2022.

Hamburger, T., McMeeking, G., Minikin, A., Birmili, W., Dall'Osto, M., O'Dowd, C., Flentje, H., Henzing, B., Junninen, H., Kristensson, A., De Leeuw, G., Stohl, A., Burkhart, J. F., Coe, H., Krejci, R., and Petzold, A.: Overview of the synoptic and pollution situation over Europe during the EUCAARI-LONGREX field campaign, Atmos. Chem. Phys., 11, 1065–1082, https://doi.org/10.5194/acp-11-1065-2011, 2011.

Hamer, P. D., Marécal, V., Hossaini, R., Pirre, M., Warwick, N., Chipperfield, M., Samah, A. A., Harris, N., Robinson, A., Quack, B., Engel, A., Krüger, K., Atlas, E., Subramaniam, K., Oram, D., Leedham, E., Mills, G., Pfeilsticker, K., Sala, S., Keber, T., Bönisch, H., Peng, L. K., Nadzir, M. S. M., Lim, P. T., Mujahid, A., Anton, A., Schlager, H., Catoire, V., Krysztofiak, G., Fühlbrügge, S., Dorf, M., and Sturges, W. T.: Modelling the chemistry and transport of bromoform within a sea breeze driven convective system during the SHIVA Campaign, Atmos. Chem. Phys. Discuss., 13, 20611–20676, https://doi.org/10.5194/acpd-13-20611-2013, 2013.

Hamer, P. D., Marecal, V., Hossaini, R., Pirre, M., Krysztofiak, G., Ziska, F., Engel, A., Sala, S., Keber, T., Bonisch, H., Atlas, E., Kruger, K., Chipperfield, M., Catoire, V., Samah, A. A., Dorf, M., Siew Moi, P., Schlager, H., and Pfeilsticker, K.: Cloud-scale modelling of the

https://doi.org/10.5194/essd-2023-82
Preprint. Discussion started: 22 March 2023


impact of deep convection on the fate of oceanic bromoform in the troposphere: A case study over the west coast of Borneo, Atmos. Chem. Phys., 21, 16955–16984, https://doi.org/10.5194/acp-21-16955-2021, 2021.

Hanke, M., Umann, B., Uecker, J., Arnold, F., and Bunz, H.: Atmospheric measurements of gas-phase HNO3 and SO2 using chemical ionization mass spectrometry during the MINATROC field campaign 2000 on Monte Cimone, Atmos. Chem. Phys., 3, 417–436, https://doi.org/10.5194/acp-3-417-2003, 2003.

Harrison, R. M., Dall'Osto, M., Beddows, D. C. S., Thorpe, A. J., Bloss, W. J., Allan, J. D., Coe, H., Dorsey, J. R., Gallagher, M., Martin, C., Whitehead, J., Williams, P. I., Jones, R. L., Langridge, J. M., Benton, A. K., Ball, S. M., Langford, B., Hewitt, C. N., Davison, B., Martin, D., Petersson, K. F., Henshaw, S. J., White, I. R., Shallcross, D. E., Barlow, J. F., Dunbar, T., Davies, F., Nemitz, E., Phillips, G. J., Helfter, C., Di Marco, C. F., and Smith, S.: Atmospheric chemistry and physics in the atmosphere of a developed megacity (London): An overview of the REPARTEE experiment and its conclusions, Atmos. Chem. Phys., 12, 3065–3114, https://doi.org/10.5194/acp-12-3065-2012, 2012.

Hegarty, J. D., Cady-Pereira, K. E., Payne, V. H., Kulawik, S. S., Worden, J. R., Kantchev, V., Worden, H. M., McKain, K., Pittman, J. V, Commane, R., Daube Jr., B. C., and Kort, E. A.: Validation and error estimation of AIRS MUSES CO profiles with HIPPO, ATom, and NOAA GML aircraft observations, Atmos. Meas. Tech., 15, 205–223, https://doi.org/10.5194/amt-15-205-2022, 2022.

Jaffe, D., Schnieder, B., and Inouye, D.: Technical note: Use of $PM_{2.5}$ to CO ratio as a tracer of wildfire smoke in urban areas, Atmos. Chem. Phys. Discuss., 2022, 1–15, https://doi.org/10.5194/acp-2022-138, 2022.

Jaffe, D. A. and Wigder, N. L.: Ozone production from wildfires: A critical review, Atmos. Environ., 51, 1–10, https://doi.org/10.1016/j.atmosenv.2011.11.063, 2012.

Kniffka, A., Knippertz, P., and Fink, A. H.: The role of low-level clouds in the West African monsoon system, Atmos. Chem. Phys., 19, 1623–1647, https://doi.org/10.5194/acp-19-1623-2019, 2019.

Knippertz, P., Coe, H., Chiu, J. C., Evans, M. J., Fink, A. H., Kalthoff, N., Liousse, C., Mari, C., Allan, R. P., Brooks, B., Danour, S., Flamant, C., Jegede, O. O., Lohou, F., and Marsham, J. H.: The DACCIWA Project: Dynamics–Aerosol–Chemistry–Cloud Interactions in West Africa, Bull. Am. Meteorol. Soc., 96, 1451–1460, https://doi.org/10.1175/BAMS-D-14-00108.1, 2015.

Krysztofiak, G., Catoire, V., Hamer, P. D., Marécal, V., Robert, C., Engel, A., Bönisch, H., Grossmann, K., Quack, B., Atlas, E., and Pfeilsticker, K.: Evidence of convective transport in tropical West Pacific region during SHIVA experiment, Atmos. Sci. Lett., 19, 1–7, https://doi.org/10.1002/asl.798, 2018.

Lelieveld, J., Butler, T. M., Crowley, J. N., Dillon, T. J., Fischer, H., Ganzeveld, L., Harder, H., Lawrence, M. G., Martinez, M., Taraborrelli, D., and Williams, J.: Atmospheric oxidation capacity sustained by a tropical forest, Nature, 452, 737–740, https://doi.org/10.1038/nature06870, 2008.

Machado, L. A. T., Calheiros, A. J. P., Biscaro, T., Giangrande, S., Dias, M. A. F. S., Cecchini, M. A., Albrecht, R., Andreae, M. O., Araujo, W. F., Artaxo, P., Borrmann, S., Braga, R., Burleyson, C., Eichholz, C. W., Fan, J., Feng, Z., Fisch, G. F., Jensen, M. P., Martin, S. T., Pöschl, U., Pöhlker, C., Pöhlker, M. L., Ribaud, J. F., Rosenfeld, D., Saraiva, J. M. B., Schumacher, C., Thalman, R., Walter, D., and Wendisch, M.: Overview: Precipitation characteristics and sensitivities to environmental conditions during GoAmazon2014/5 and ACRIDICON-CHUVA, Atmos. Chem. Phys., 18, 6461–6482, https://doi.org/10.5194/acp-18-6461-2018, 2018.

Mallet, M., Dulac, F., Formenti, P., Nabat, P., Sciare, J., Roberts, G., Pelon, J., Ancellet, G., Tanré, D., Parol, F., Denjean, C., Brogniez, G., di Sarra, A., Alados-Arboledas, L., Arndt, J., Auriol, F., Blarel, L., Bourrianne, T., Chazette, P., Chevaillier, S., Claeys, M., D'Anna, B., Derimian, Y., Desboeufs, K., Di Iorio, T., Doussin, J.-F., Durand, P., Féron, A., Freney, E., Gaimoz, C., Goloub, P., Gómez-Amo, J. L., Granados-Muñoz, M. J., Grand, N., Hamonou, E., Jankowiak, I., Jeannot, M., Léon, J.-F., Maillé, M., Mailler, S., Meloni, D., Menut, L., Momboisse, G., Nicolas, J., Podvin, T., Pont, V., Rea, G., Renard, J.-B., Roblou, L., Schepanski, K., Schwarzenboeck, A., Sellegri, K., Sicard, M., Solmon, F., Somot, S., Torres, B., Totems, J., Triquet, S., Verdier, N., Verwaerde, C., Waquet, F., Wenger, J., and Zapf, P.: Overview of the Chemistry-Aerosol Mediterranean Experiment/Aerosol Direct Radiative Forcing on the Mediterranean Climate (ChArMEx/ADRIMED) summer 2013 campaign, Atmos. Chem. Phys., 16, 455–504, https://doi.org/10.5194/acp-16-455-2016, 2016.

Ravi Kant Pathak, Wai Shing Wu, and Tao Wang: Summertime $PM_{2.5}$ ionic species in four major cities of China: nitrate formation in an ammonia-deficient atmosphere, Atmos. Chem. Phys., 9, 1711–1722, https://doi.org/10.5194/acpd-8-11487-2008, 2009.



Ricaud, P., Zbinden, R., Catoire, V., Brocchi, V., Dulac, F., Hamonou, E., Canonici, J. C., El Amraoui, L., Massart, S., Piguet, B., Dayan, U., Nabat, P., Sciare, J., Ramonet, M., Delmotte, M., Di Sarra, A., Sferlazzo, D., Di Iorio, T., Piacentino, S., Cristofanelli, P., Mihalopoulos, N., Kouvarakis, G., Pikridas, M., Savvides, C., Mamouri, R. E., Nisantzi, A., Hadjimitsis, D., Attié, J. L., Ferré, H., Kangah, Y., Jaidan, N., Guth, J., Jacquet, P., Chevrier, S., Robert, C., Bourdon, A., Bourdinot, J. F., Etienne, J. C., Krysztofiak, G., and Theron, P.: The GLAM airborne campaign across the Mediterranean Basin, Bull. Am. Meteorol. Soc., 99, 361–380, https://doi.org/10.1175/BAMS-D-16-0226.1, 2018.

Ryerson, T. B., Andrews, A. E., Angevine, W. M., Bates, T. S., Brock, C. A., Cairns, B., Cohen, R. C., Cooper, O. R., De Gouw, J. A., Fehsenfeld, F. C., Ferrare, R. A., Fischer, M. L., Flagan, R. C., Goldstein, A. H., Hair, J. W., Hardesty, R. M., Hostetler, C. A., Jimenez, J. L., Langford, A. O., McCauley, E., McKeen, S. A., Molina, L. T., Nenes, A., Oltmans, S. J., Parrish, D. D., Pederson, J. R., Pierce, R. B., Prather, K., Quinn, P. K., Seinfeld, J. H., Senff, C. J., Sorooshian, A., Stutz, J., Surratt, J. D., Trainer, M., Volkamer, R., Williams, E. J., and Wofsy, S. C.: The 2010 California Research at the Nexus of Air Quality and Climate Change (CalNex) field study, J. Geophys. Res. Atmos., 118, 5830–5866, https://doi.org/10.1002/jgrd.50331, 2013.

Sellers, P., Hall, F., Ranson, K. J., Margolis, H., Kelly, B., Baldocchi, D., den Hartog, G., Cihlar, J., Ryan, M. G., Goodison, B., Crill, P., Lettenmaier, D., and Wickland, D. E.: The Boreal Ecosystem–Atmosphere Study (BOREAS): An Overview and Early Results from the 1994 Field Year, Bull. Am. Meteorol. Soc., 76, 1549–1577, https://doi.org/10.1175/1520-0477(1995)076<1549:TBESAO>2.0.CO;2, 1995.

Shi, Z., Vu, T., Kotthaus, S., Harrison, R. M., Grimmond, S., Yue, S., Zhu, T., Lee, J., Han, Y., Demuzere, M., Dunmore, R. E., Ren, L., Liu, D., Wang, Y., Wild, O., Allan, J., Joe Acton, W., Barlow, J., Barratt, B., Beddows, D., Bloss, W. J., Calzolai, G., Carruthers, D., Carslaw, D. C., Chan, Q., Chatzidiakou, L., Chen, Y., Crilley, L., Coe, H., Dai, T., Doherty, R., Duan, F., Fu, P., Ge, B., Ge, M., Guan, D., Hamilton, J. F., He, K., Heal, M., Heard, D., Nicholas Hewitt, C., Hollaway, M., Hu, M., Ji, D., Jiang, X., Jones, R., Kalberer, M., Kelly, F. J., Kramer, L., Langford, B., Lin, C., Lewis, A. C., Li, J., Li, W., Liu, H., Liu, J., Loh, M., Lu, K., Lucarelli, F., Mann, G., McFiggans, G., Miller, M. R., Mills, G., Monk, P., Nemitz, E., O'Connor, F., Ouyang, B., Palmer, P. I., Percival, C., Popoola, O., Reeves, C., Rickard, A. R., Shao, L., Shi, G., Spracklen, D., Stevenson, D., Sun, Y., Sun, Z., Tao, S., Tong, S., Wang, Q., Wang, W., Wang, X., Wang, X., Wang, Z., Wei, L., Whalley, L., Wu, X., Wu, Z., Xie, P., Yang, F., Zhang, Q., Zhang, Y., Zhang, Y., and Zheng, M.: Introduction to the special issue "in-depth study of air pollution sources and processes within Beijing and its surrounding region (APHH-Beijing)," Atmos. Chem. Phys., 19, 7519–7546, https://doi.org/10.5194/acp-19-7519-2019, 2019.

Spackman, J. R., Gao, R. S., Neff, W. D., Schwarz, J. P., Watts, L. A., Fahey, D. W., Holloway, J. S., Ryerson, T. B., Peischl, J., and Brock, C. A.: Aircraft observations of enhancement and depletion of black carbon mass in the springtime Arctic, Atmos. Chem. Phys., 10, 9667–9680, https://doi.org/10.5194/acp-10-9667-2010, 2010.

Tang, Y. S., Flechard, C. R., Dämmgen, U., Vidic, S., Djuricic, V., Mitosinkova, M., Uggerud, H. T., Sanz, M. J., Simmons, I., Dragosits, U., Nemitz, E., Twigg, M., van Dijk, N., Fauvel, Y., Sanz, F., Ferm, M., Perrino, C., Catrambone, M., Leaver, D., Braban, C. F., Cape, J. N., Heal, M. R., and Sutton, M. A.: Pan-European rural monitoring network shows dominance of $NH_3$ gas and $NH_4NO_3$ aerosol in inorganic atmospheric pollution load, Atmos. Chem. Phys., 21, 875–914, https://doi.org/10.5194/acp-21-875-2021, 2021.

Taylor, J. W., Haslett, S. L., Bower, K., Flynn, M., Crawford, I., Dorsey, J., Choularton, T., Connolly, P. J., Hahn, V., Voigt, C., Sauer, D., Dupuy, R., Brito, J., Schwarzenboeck, A., Bourriane, T., Denjean, C., Rosenberg, P., Flamant, C., Lee, J. D., Vaughan, A. R., Hill, P. G., Brooks, B., Catoire, V., Knippertz, P., and Coe, H.: Aerosol influences on low-level clouds in the West African monsoon, Atmos. Chem. Phys., 19, 8503–8522, https://doi.org/10.5194/acp-19-8503-2019, 2019.

Wizenberg, T., Strong, K., Walker, K., Lutsch, E., Borsdorff, T., and Landgraf, J.: Intercomparison of CO measurements from TROPOMI, ACE-FTS, and a high-Arctic ground-based Fourier transform spectrometer, Atmos. Meas. Tech., 14, 7707–7728, https://doi.org/10.5194/amt-14-7707-2021, 2021.

Xue, C., Zhang, C., Ye, C., Liu, P., Catoire, V., Krysztofiak, G., Chen, H., Ren, Y., Zhao, X., Wang, J., Zhang, F., Zhang, C., Zhang, J., An, J., Wang, T., Chen, J., Kleffmann, J., Mellouki, A., and Mu, Y.: HONO Budget and Its Role in Nitrate Formation in the Rural North China Plain, Environ. Sci. Technol., 54, 11048–11057, https://doi.org/10.1021/acs.est.0c01832, 2020.